Contemporary Mathematics
http://ojs.wiserpub.com/index.php/CM/

Research Article

Exact Time-Dependent Thermodynamic Relationships for a Brownian Particle Navigating Complex Networks

Mesfin Asfaw Taye

West Los Angeles College, Science Division 9000 Overland Ave, Culver City, CA 90230, USA
E-mail: tayem@wlac.edu

Received: 7 June 2024; **Revised:** 1 August 2024; **Accepted:** 6 August 2024

Abstract: The thermodynamic characteristics of systems driven out of equilibrium are examined for M Brownian ratchets organized in a complex network. The precise time-dependent solution reveals that the entropy S, entropy production $e_p(t)$, and entropy extraction $h_d(t)$ of the system in complex networks increase with system size, which is plausible as these thermodynamic quantities display extensive properties. In other words, as the number of lattice sites increases, the entropy S, entropy production $e_p(t)$, and entropy extraction $h_d(t)$ increase, demonstrating that these complex networks cannot be reduced to the corresponding one-dimensional lattice. Conversely, the rates for thermodynamic quantities such as velocity V, entropy production rate $\dot{e}_p(t)$, and entropy extraction rate $\dot{h}_d(t)$ become independent of the network size in the long-term limit. The exact analytic results also indicate that the free energy decreases with system size. The model system is further analyzed by incorporating heat transfer via kinetic energy. Since heat exchange via kinetic energy does affect the energy extraction rate, the heat dumped to the cold reservoirs also contributes to internal entropy production. Consequently, such systems exhibit a higher degree of irreversibility. The thermodynamic features of a system operating between hot and cold baths are also compared and contrasted with a system functioning in a heat bath where temperature varies linearly along the reaction coordinate. Regardless of the network arrangements, the entropy, entropy production, and extraction rates are significantly larger for the linearly varying temperature case than for a system operating between hot and cold baths.

***Keywords*:** brownian motion, time-dependent thermodynamics, complex networks, stochastic processes, nonequilibrium system

MSC: 60J65 82C31

1. Introduction

Thermodynamics is an important discipline that has historically began to study how heat and matter exchange from one system to another system. Since its relevance to science and technology is considerably high, the study of thermodynamics systems have obtained considerable attention. Particularly, exploring the dependence on entropy production e_p is vital since not only it signifies the degree of irreversibility of a given system but also serves as a fundamental limit regarding the efficiency of thermodynamic systems. As indicated by the second law of thermodynamics, $e_p \geq 0$ signifies that systems always maximize their entropy production during an irreversible process and $e_p = 0$ for

DOI: https://doi.org/10.37256/cm.5420245113

reversible processes [1, 2]. In the past decades, several frameworks have been developed to tackle how entropy production, as well as entropy production rates behave. Some pioneering work in this regard includes Onsager's reciprocity theory [3, 4] which applies to a system operating near a linear response regime.

Systems that are genuinely far from equilibrium also have obtained considerable attention see for example the works [5–21]. Some of these studies have explored the dependence of the thermodynamic quantities either by considering classical systems [22, 23] or systems that operate in the quantum realm [24–26]. Since the Boltzmann-Gibbs nonequilibrium entropy along with the entropy balance equation still remain valid for systems that are far from equilibrium, exploiting this property, many theoretical studies have been conducted to study the entropy production in terms of the local probability density and transition probability rate. For discrete systems, employing the master equation approach, the dependence of entropy production has been studied in the works [5–9]. For continuous systems, via the Fokker-Planck equation, several thermodynamics relations have been derived [11, 12, 17, 27, 28]. The method of calculating entropy production and extraction rates at the ensemble level by first analyzing thermodynamic relations at the trajectory level was introduced in the work [10]. Alternatively, many thermodynamic relations that derived via stochastic thermodynamics were reconfirmed under time reversal operation [29, 30]. At a single trajectory level, various thermodynamics relations have been derived via the fluctuation theorem [31–33]. The recent work [34] also indicates that for non-Markovian systems, the entropy production rate can be negative. All of these studies have explored entropy production based on full dynamical equations. However, inferring the entropy production for short experimental data is also vital but challenging since such studies lack a complete picture of the nature of interactions. In this regard, the recent fundamental relation called the thermodynamic uncertainty relation (TUR) sheds light on obtaining the expression for the entropy production from a given time series data [35–38]. Recently, TUR has been generalized to study the entropy production for periodically driven systems [38]. Most recently, considering a single thermal ratchet, the general expressions for free energy, entropy production, as well as entropy extraction rates, are derived for a system that is genuinely driven out of equilibrium by time-independent force as well as by spatially varying thermal background [39].

In this work, extending our previous study [39], we further study the thermodynamic features of a single Brownian particle that walks along M Brownian ratchets arranged in a complex network. Each ratchet potential is either coupled with the hot and cold reservoirs or a heat bath where its temperature decreases linearly along the reaction coordinate. The analytical result depicts that the rate for the thermodynamic quantities such as the velocity V, entropy production $\dot{e}_p(t)$ as well as entropy extraction $\dot{h}_d(t)$ are independent of the network size at steady state as reconfirmed by complex generating functions. On the contrary, the thermodynamic relations such as the entropy S, entropy production $e_p(t)$, and entropy extraction $h_d(t)$ of the system step up with the network size M even at a steady state. We then further, study the system by including heat transfer via kinetic energy. Since the heat exchange via kinetic energy does affect the energy dissipation rate, the heat dumped to the cold reservoirs contributes also to the internal entropy production. This implies that such a system exhibits a higher degree of irreversibility as long as a distinct temperature is retained between the hot and cold heat baths. The thermodynamic properties of systems that operate between the hot and cold baths are also compared and contrasted with a system that operates in a heat bath where its temperature varies linearly along with the reaction coordinate. Regardless of the network size M, the entropy, entropy production, and extraction rates are considerably larger for the linearly varying temperature case than a system that operates between the hot and cold baths revealing such systems are inherently irreversible.

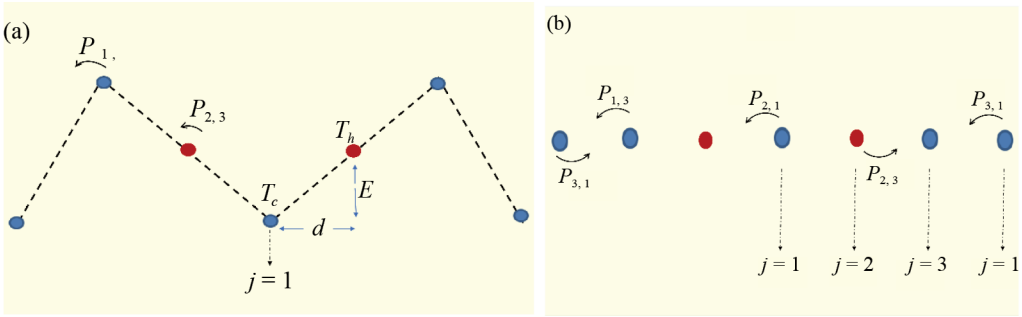

Figure 1. (Color online) (a) Schematic diagram (Side view) for a Brownian particle walking in two discrete ratchet potentials with the load. Sites with red circles are coupled to the hot reservoir (T_h) while sites with blue circles are coupled to the cold reservoir (T_c). Site 1 is labeled explicitly and d is the lattice spacin; (b) A Brownian particle (top view) walking in two discrete ratchet potentials with a load. Sites with red circles are coupled to the hot reservoir (T_h) while sites with blue circles are coupled to the cold reservoir (T_c)

The model system presented in this study is crucial for examining the thermodynamic properties of Brownian particles within complex networks. For instance, protein-based molecular motors such as kinesin, myosin, and dynein navigate through complex networks. Additionally, nanorobots, which function as artificial Brownian motors, are engineered to achieve unidirectional motion on two-dimensional surfaces. Furthermore, numerous physically significant problems, such as the diffusion of impurities (donors) within semiconductor layers, require comprehensive two-dimensional and three-dimensional treatment.

We want to emphasize that a higher entropy is observed for a linearly decreasing temperature case than a Brownian particle that operates between the hot and cold baths. Consequently, systems that operate in a linearly decreasing temperature heat bath, have very low efficiency but a higher velocity. Thus such a thermal arrangement is beneficial in designing a device that channels a Brownian particle fast along the reaction coordinate. A Brownian particle that operates between two heat baths has a higher efficiency but a lower velocity in comparison with a linearly decreasing temperature case. Thus such a model system is advantageous if the sole purpose is to design an efficient Brownian motor. For all thermal arrangements, the particle attains a faster velocity whenever the network size M increases. This suggests that by properly arranging the model ingredient prior to the motor operation, a specific task can be accomplished. Thus the exactly solvable model presented in this work helps in designing artificial Brownian motors such as nanorobots.

The rest of the paper is organized as follows: in Section II, we present the model. The role of time is explored for a Brownian particle moving on M Brownian ratchets arranged in a complex network where each ratchet potential is coupled with the hot and cold baths. The model system is further explored by including heat transfer via kinetic energy. An alternative derivation for steady-state thermodynamic quantities via complex generating functions is also presented. In section III, we study the thermodynamic relations for Brownian particle that operates on M Brownian ratchets are arranged in a complex network. Each ratchet potential is coupled with a heat bath where its temperature decreases linearly along the reaction coordinate. Section IV deals with the summary and conclusion.

2. Brownian particle operating in a networks that coupled with the hot and cold reservoirs

2.1 *The model*

The Brownian particle undergoes a biased random walk along a discrete ratchet potential with load that coupled with the temperature

$$T_j = \begin{cases} T_h, & \text{for site } j = 0; \\ T_c, & \text{for sites } j = 1 \text{ and } j = 2; \end{cases} \tag{1}$$

as shown in Figure 1a and 1b. The potential barrier height $E > 0$, f denotes the load and j is an integer. T_h and T_c represent the temperature for the hot and cold reservoirs, respectively. The lattice has spacing d and in one cycle, the particle walks a net displacement of three lattice sites.as shown in Figure 1. The potential $E > 0$, f denotes the load and i is an integer that runs from $-\infty$ to ∞. T_h and T_c designate the temperature for the hot and cold reservoirs, respectively. Moreover, d denotes the lattice spacing d and in one cycle, the particle walks a net displacement of three lattice sites as shown in Figure 1. The jump probability from site i to $i+1$ is given by $\Gamma e^{-\Delta E/k_B T_i}$ where $\Delta E = U_{i+1} - U_i$ and Γ is the probability attempting a jump per unit time. k_B designates the Boltzmann constant and hereafter k_B, Γ and d are considered to be a unity. Obeying the metropolis algorithm when $\Delta E \leq 0$, the jump definitely takes place while $\Delta E > 0$ the jump takes place with probability $\exp(-\Delta E/T_i)$ [18].

It is also of practical interest to investigate the thermodynamic feature of M ratchet potentials arranged in a lattice (each potential has a similar arrangement as shown in Figure 2a and 2b. This is because most practical problems such as neural system, cardiac system as well as impurities (donors) diffusion along the semiconductor layer require 2D and 3D analysis. As shown in Figure 2a, each ratchet potential shares a common hot bath and a cold bath at the other end. When a periodic boundary condition is imposed, such arrangements can be mapped into the network depicted in Figure 2b. For instance, the geometry of the networks shown in Figure 2a and 2b are essentially the same (when $M = 4$) if one binds the nodes A, B, C, D of Figure 2a together (when a periodic boundary condition is imposed).

For a Brownian particle that moves in a discrete lattice, its dynamics is governed by the master equation

$$\frac{dP_n}{dt} = \sum_{n \neq n'} \left(P_{nn'} p_{n'} - P_{n'n} p_n\right), \; n, \; n' = 1, \; 2, \; 3 \tag{2}$$

where $P_{n'n}$ is the transition probability rate at which the system, originally in state n, makes a transition to state n'. $P_{n'n}$ is given by the Metropolis rule [22]. Equation (2) can be rewritten as

$$\frac{d\vec{p}}{dt} = \mathbf{P}\vec{p}. \tag{3}$$

Note that mathematically, Brownian motion can be described using the Langevin equation, Master equation or the Fokker-Planck equation. These equations account for the forces acting on a particle and the resulting motion due to thermal fluctuations. The expression for $\mathbf{P}$ can be evaluated for any M. For instance, for a single ratchet potential $M = 1$, $\mathbf{P}$ is a 3 by 3 matrix which is given by

$$\mathbf{P} = \begin{pmatrix} \frac{-\mu a^2 - \mu^2}{2a} & \frac{1}{2} & \frac{1}{2} \\ \frac{\mu a}{2} & \frac{-1-\nu b}{2} & \frac{1}{2} \\ \frac{\mu^2}{2a} & \frac{\nu b}{2} & -1 \end{pmatrix}. \tag{4}$$

For two ratchet potentials ($M = 2$), $\mathbf{P}$ has a form

$$\mathbf{P}=\begin{pmatrix} \frac{-2\mu a^2-2\mu^2}{2a} & \frac{1}{2} & \frac{1}{2} & \frac{1}{2} & \frac{1}{2} \\ \frac{\mu a}{2} & \frac{-1-\nu b}{2} & 0 & \frac{1}{2} & 0 \\ \frac{\mu a}{2} & 0 & \frac{-1-\nu b}{2} & 0 & \frac{1}{2} \\ \frac{\mu^2}{2a} & \frac{\nu b}{2} & 0 & -1 & 0 \\ \frac{\mu^2}{2a} & 0 & \frac{\nu b}{2} & 0 & -1 \end{pmatrix} \tag{5}$$

while for $M=3$ and $M=4$ case, one finds

$$\mathbf{P}=\begin{pmatrix} \frac{-3\mu a^2-3\mu^2}{2a} & \frac{1}{2} & \frac{1}{2} & \frac{1}{2} & \frac{1}{2} & \frac{1}{2} & \frac{1}{2} \\ \frac{\mu a}{2} & \frac{-1-\nu b}{2} & 0 & 0 & \frac{1}{2} & 0 & 0 \\ \frac{\mu a}{2} & 0 & \frac{-1-\nu b}{2} & 0 & 0 & \frac{1}{2} & 0 \\ \frac{\mu a}{2} & 0 & 0 & \frac{-1-\nu b}{2} & 0 & 0 & \frac{1}{2} \\ \frac{\mu}{2a} & \frac{\nu b}{2} & 0 & 0 & -1 & 0 & 0 \\ \frac{\mu^2}{2a} & 0 & \frac{\nu b}{2} & 0 & 0 & -1 & 0 \\ \frac{\mu^2}{2a} & 0 & 0 & \frac{\nu b}{2} & 0 & 0 & -1 \end{pmatrix} \tag{6}$$

and

$$\mathbf{P}=\begin{pmatrix} \frac{-4\mu a^2-4\mu^2}{2a} & \frac{1}{2} & \frac{1}{2} & \frac{1}{2} & \frac{1}{2} & \frac{1}{2} & \frac{1}{2} & \frac{1}{2} & \frac{1}{2} \\ \frac{\mu a}{2} & \frac{-1-\nu b}{2} & 0 & 0 & 0 & \frac{1}{2} & 0 & 0 & 0 \\ \frac{\mu a}{2} & 0 & \frac{-1-\nu b}{2} & 0 & 0 & 0 & \frac{1}{2} & 0 & 0 \\ \frac{\mu a}{2} & 0 & 0 & \frac{-1-\nu b}{2} & 0 & 0 & 0 & \frac{1}{2} & 0 \\ \frac{\mu a}{2} & 0 & 0 & 0 & \frac{-1-\nu b}{2} & 0 & 0 & 0 & \frac{1}{2} \\ \frac{\mu^2}{2a} & \frac{\nu b}{2} & 0 & 0 & 0 & -1 & 0 & 0 & 0 \\ \frac{\mu^2}{2a} & 0 & \frac{\nu b}{2} & 0 & 0 & 0 & -1 & 0 & 0 \\ \frac{\mu^2}{2a} & 0 & 0 & \frac{\nu b}{2} & 0 & 0 & 0 & -1 & 0 \\ \frac{\mu^2}{2a} & 0 & 0 & 0 & \frac{\nu b}{2} & 0 & 0 & 0 & -1 \end{pmatrix}. \tag{7}$$

Here $\mu=e^{-E/T_c}$, $\nu=e^{-E/T_h}$, $a=e^{-f/T_c}$ and $b=e^{-f/T_h}$. In Appendix A, the expressions for the probability are presented for the cases $M=1$ and $M=2$. The escaping rates

$$P_{21} = \frac{1}{2M} e^{-(E+f)/T_c},\ P_{12} = \frac{1}{2},\ P_{32} = \frac{1}{2} e^{-(E+f)/T_h}$$

$$P_{23} = \frac{1}{2},\ P_{13} = \frac{1}{2},\ P_{31} = \frac{1}{2M} e^{-(2E-f)/T_c} \tag{8}$$

depend on M. While solving the model system, we employ periodic boundary conditions whereby a particle exiting one side of the network re-enters from the opposite side. It is assumed that the time scale is significantly larger than the microscopic collision times yet small relative to the timescale of macroscopic changes. Thermal fluctuations are modeled as random forces acting on the particles, typically following a Gaussian distribution. Additionally, in the presence of an external force or nonuniform thermal arrangements, a unidirectional current is achieved.

When solving the master equation for both thermal arrangements, idealized conditions are assumed, such as no heat losses to the surroundings except between the two reservoirs. The assumption of a linear temperature gradient or piecewise thermal arrangement is a simplification. In a real experimental setup, having such thermal arrangements at a nanoscopic or microscopic scale is a daunting task.

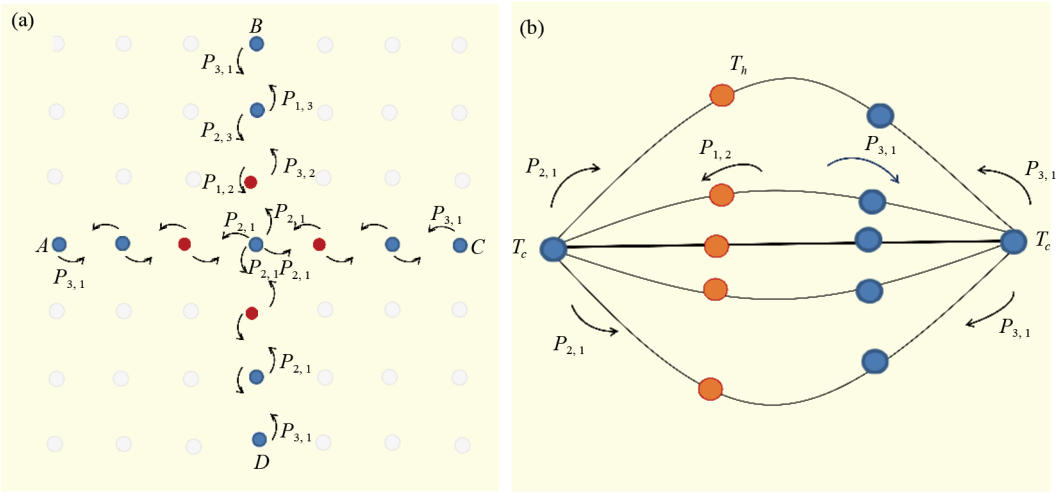

Figure 2. (Color online) (a) Top view of four thermal ratchets arranged in a lattice. Each ratchet potential has four lattice sites. Sites with red circles are coupled to the hot reservoir (T_h) while sites with blue circles are coupled to the cold reservoir (T_c). The hot bath for the four Brownian ratchets are located at the center; (b) M ratchet potentials arranged in a loop where each ratchet potentials share a common cold bath and a cold bath at the other end. Each ratchet potential has four lattice sites as shown in Figure 2. Sites with red circles are coupled to the hot reservoir (T_h) while sites with blue circles are coupled to the cold reservoir (T_c). The hot bath for the M Brownian ratchets are located on the left side. The geometry of networks shown in Figure 2a and 2b are essentially the same (when $M = 4$) if one binds the nodes A, B, C, D of Figure 6b together (when a periodic boundary condition is imposed)

For a Brownian particle that moves along one or two dimensional discrete ratchet potential, the Boltzmann-Gibbs entropy relation

$$S[p_i(t)] = -\sum_{i=1}^{3} p_i \ln p_i, \tag{9}$$

remains valid even when the system is far from equilibrium. The entropy extraction rate $\dot{h}_d(t)$ can be rewritten in terms of local probability density and transition probability rate as

$$\begin{aligned}\dot{h}_d(t) =& \frac{-\dot{Q}_h(t)}{T_h} + \frac{\dot{Q}_c(t)}{T_c} \\ =& \sum_{i>j} (p_i P_{ji} - p_j P_{ij}) \ln\left(\frac{P_{ji}}{P_{ij}}\right) \\ =& \sum_{i>j} (p_i P_{ji} - p_j P_{ij}) \ln\left(\frac{p_i P_{ji}}{p_j P_{ij}}\right) - \sum_{i>j} (p_i P_{ji} - p_j P_{ij}) \ln\left(\frac{p_i}{p_j}\right) \\ =& \dot{e}_p(t) - \dot{S}(t) \end{aligned} \tag{10}$$

where

$$\dot{e}_p(t) = \sum_{i>j} (p_i P_{ji} - p_j P_{ij}) \ln\left(\frac{p_i P_{ji}}{p_j P_{ij}}\right) \tag{11}$$

and

$$\dot{S}(t) = \sum_{i>j} (p_i P_{ji} - p_j P_{ij}) \ln\left(\frac{p_i}{p_j}\right). \tag{12}$$

Here $\dot{e}_p(t)$ and $\dot{S}(t)$ designate the entropy production rate and the rate of total entropy, respectively while $\dot{Q}_h(t)$ and $\dot{Q}_c(t)$ denote the heat per unit time taken from the hot reservoir and the heat per unit time given to cold reservoir, respectively.

After calculating the expressions for $\dot{S}(t)$, $\dot{e}_p(t)$ and $\dot{h}_d(t)$ as a function of t, the analytic expressions for the change in entropy production, heat dissipation and total entropy can be found analytically via $\Delta h_d(t) = \int_{t_0}^{t} \left(\dot{h}_d(t)\right) dt$, $\Delta e_p(t) = \int_{t_0}^{t} \left(\dot{e}_p(t)\right) dt$, and $\Delta S(t) = \int_{t_0}^{t} \left(\dot{S}(t)\right) dt$ where $\Delta S(t) = \Delta e_p(t) - \Delta h_d(t)$. Once again, in the absence of load f, in the limit $T_h \to T_c$ and when $E = 0$, for both cases, one finds $\Delta h_d(t) = 0$,

In terms of local probability density and transition probability, the heat dissipation rate can be given as

$$\begin{aligned}\dot{H}_d(t) =& \sum_{i>j} T_j (p_i P_{ji} - p_j P_{ij}) \ln\left(\frac{P_{ji}}{P_{ij}}\right) \\ =& \sum_{i>j} T_j (p_i P_{ji} - p_j P_{ij}) \ln\left(\frac{p_i P_{ji}}{p_j P_{ij}}\right) - \sum_{i>j} T_j (p_i P_{ji} - p_j P_{ij}) \ln\left(\frac{p_i}{p_j}\right) \\ =& \dot{E}_p(t) - \dot{S}^T(t) \end{aligned} \tag{13}$$

where

$$\dot{E}_p(t) = \sum_{i>j} T_j(p_i P_{ji} - p_j P_{ij}) \ln\left(\frac{p_i P_{ji}}{p_j P_{ij}}\right) \tag{14}$$

and

$$\dot{S}^T(t) = \sum_{i>j} T_j(p_i P_{ji} - p_j P_{ij}) \ln\left(\frac{p_i}{p_j}\right). \tag{15}$$

Our next objective is to write the expression for the free energy in terms of $\dot{E}_p(t)$ and $\dot{H}_d(t)$ where $\dot{E}_p(t)$ and $\dot{H}_d(t)$ are the terms that are associated with $\dot{e}_p(t)$ and $\dot{h}_d(t)$ except the temperature T_j.

The second law of thermodynamics can be written as $\Delta S^T(t) = \Delta E_p(t) - \Delta H_d(t)$ where $\Delta S^T(t)$, $\Delta E_p(t)$ and $\Delta H_d(t)$ are very lengthy expressions which can be evaluated via $\Delta H_d = \int_{t_0}^{t} \left(\dot{H}_d(t)\right) dt$, $\Delta E_p(t) = \int_{t_0}^{t} \left(\dot{E}_p(t)\right) dt$ and $\Delta S^T(t) = \int_{t_0}^{t} (\dot{S}^T(t)) dt$. On the other hand, the total internal energy $U(t)$ is the sum of the internal energies

$$U[p_i(t)] = \sum_{i=1}^{3} p_i u_i \tag{16}$$

while the change in the internal energy is given by $\Delta U(t) = U[p_i(t)] - U[p_i(0)]$. We also verify the first law of thermodynamics

$$\dot{U}[P_i(t)] = -\sum_{i>j} (p_i P_{ji} - p_j P_{ij})(u_i - u_j)$$

$$= -(\dot{H}_d(t) + fV(t)) \tag{17}$$

where the net velocity $V(t)$ at any time t is the difference between the forward $V_i^+(t)$ and backward $V_i^-(t)$ velocities at each site i. Next let us find the expression for the free energy dissipation rate $\dot{F}$. For the isothermal case, the free energy is given by $F = U - TS$ and next we adapt this relationship to nonisothermal case to write

$$\dot{F}(t) = \dot{U} - \dot{S}^T(t). \tag{18}$$

Substituting Eqs. (10) and (17) in Eq. (18) leads to

$$\dot{F}(t) + \dot{E}_p(t) = \dot{U}(t) + \dot{H}_d(t) = -fV(t) \tag{19}$$

which is the second law of thermodynamics. Note that in the absence of load, $\dot{U}(t) = -\dot{H}_d(t)$ and consequently $\dot{E}_p(t) = -\dot{F}(t)$. The change in the free energy can be written as

$$\Delta F(t) = -\int_{t_0}^{t} \left(fV(t) + \dot{E}_p(t)\right) dt$$

$$= \int_{t_0}^{t} \left(\dot{U}(t) + \dot{H}_d(t) - \dot{E}_p(t)\right) dt$$

$$= \Delta U + \Delta H_d - \Delta E_p. \tag{20}$$

2.2 *Entropy, entropy production and extraction rates*

The net velocity $V(t)$ at any time t is the difference between the forward $V_i^+(t)$ and backward $V_i^-(t)$ velocities at each site i. For instance, for $M = 2$ cases, the velocity can be calculated as

$$V(t) = \sum_{i=1}^{3} (V_i^+(t) - V_i^-(t))$$

$$= (p_1 P_{21} - p_2 P_{12}) + (p_2 P_{32} - p_3 P_{23}) +$$

$$(p_3 P_{13} - p_1 P_{31}) + (p_1 P'_{21} - p'_2 P'_{12}) + (p'_2 P'_{32} - p'_3 P'_{23}) + (p'_3 P'_{13} - p_1 P'_{31}). \tag{21}$$

Because closed-form expressions for $V(t)$, $\dot{S}(t)$, $\dot{e}_p(t)$ and $\dot{h}_d(t)$ as a function of t is obtained, one can explore the dependence of other physical quantities as a function of time. To increase the readability of this paper, only the thermodynamic expressions up to $M = 4$ will be shown in this paper.

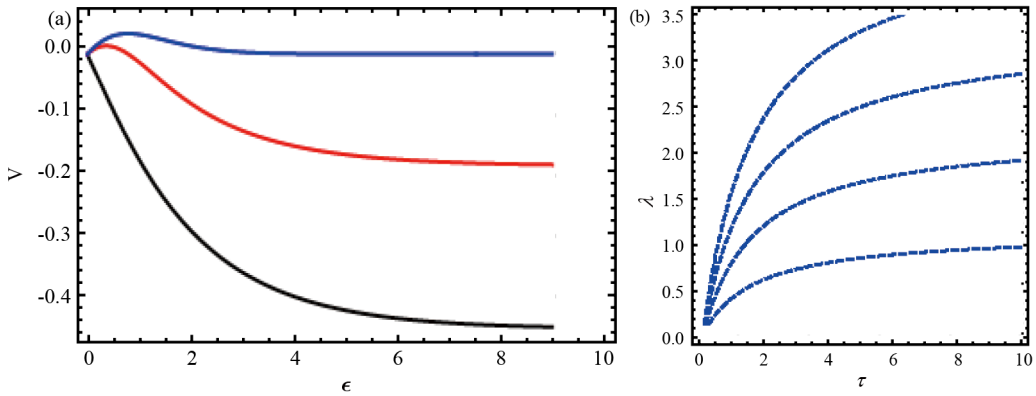

Figure 3. (Color online) (a) Particle velocity V as a function of ε is plotted via Eq. (21) for fixed $M = 4$ and $\tau = 2.0$. The load is fixed as $\lambda = 0$, $\lambda = 0.5$, and $\lambda = 1.0$ from the top to bottom; (b) Phase space at which the velocity $V = 0$ is plotted as a function of λ and τ. The potential height is fixed as $\varepsilon = 8.0$, $\varepsilon = 6.0$, $\varepsilon = 4.0$ and $\varepsilon = 2.0$ from top to bottom

Hereafter, whenever we plot the figures, we use the following dimensionless load $\lambda = f/T_c$, barrier height $\varepsilon = E/T_c$ and dimensionless temprature $\tau = T_h/T_c$.

The velocity. The dependence of the velocity on model parameters is explored as a function of time. The time t dictates the magnitude and direction of the velocity. For small t, the net particle flow is in the reverse direction (negative).

As time increases, the direction of V is reversed. In Figure 3a, we plot the velocity V as a function of ε. The figure depicts that the particle manifests a peak velocity at a particular barrier height ε^{max}. At this particular height, the engine operates with maximum power. Phase space at which the velocity $V = 0$ is plotted in Fig. 3b as a function of λ and τ. In the figure, the potential height is fixed as $\varepsilon = 8.0$, $\varepsilon = 6.0$, $\varepsilon = 4.0$, and $\varepsilon = 2.0$ from top to bottom.

The velocity increases as the number of ratchet potentials (M) steps up. At a steady state, the velocity approaches the same value regardless of the number of ratchet potentials arranged in the lattice. At steady state, for all M, the velocity approaches

$$V = \frac{3\left(e^{E/T_c} - e^{\frac{2f}{T_c}+\frac{E}{T_h}+\frac{f}{T_h}}\right)}{2\left(e^{E/T_c} + e^{\frac{2f}{T_c}} + e^{\frac{2E+f}{T_c}}\right)\left(1+2e^{\frac{E+f}{T_h}}\right)}. \tag{22}$$

At stall force

$$f^s = \frac{E(\frac{T_h}{T_c}-1)}{(\frac{2T_h}{T_c}+1)} \tag{23}$$

the velocity approaches zero.

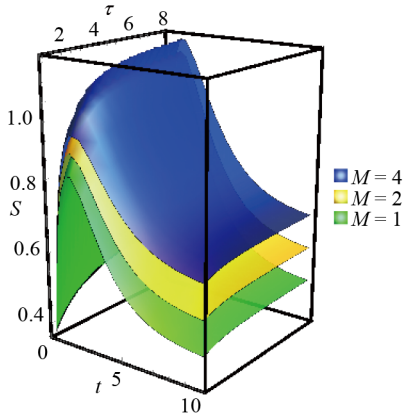

Figure 4. (Color online) The entropy $S(t)$ as a function of t and τ evaluated analytically via Eq. (9) for a given $\varepsilon = 2.0$ and $f = 0.0$. In the figure, M is fixed as $M = 4$, $M = 2$, and $M = 1$ from top to bottom, respectively

At this point, we want to emphasize that the model system not only serves as an important tool to calculate the velocity for thermally driven motors but also for isothermal motors (protein-based molecular motors) such as Myosins, Kinesin, and Dynein. When the motor operates in isothermal baths, the engines undergo unidirectional motion by utilizing chemical energy. For the isothermal case $T_h = T_c$, the load only acts as the symmetry-breaking field. Thus in the presence of load, the motor attains a unidirectional velocity depending on the magnitude of the load.

The total entropy. The fundamental entropy relation

$$S[p_i(t)] = -\sum_{i=1}^{3} p_i \ln p_i, \tag{24}$$

for the system which is far from equilibrium can be derived by substituting $\dot{Q}_h(t)$ and $\dot{Q}_c(t)$ into Eq. (10). Here care must be taken that the change in the entropy $\Delta S = \Delta e_p - \Delta h_d$ reflects the system properties while the entropy production Δe_p signifies the spontaneous change that the system undergoes. At this point, it is important to acknowledge Prigogine's theory [40], which demonstrates that for a system out of equilibrium, the entropy balance equation is given by $dS = d_eS + d_iS$ where dS represents the total entropy variation, d_eS is the entropy flow to the surroundings and d_iS is the entropy production. Our entropy balance equation $\Delta S = \Delta e_p - \Delta h_d$ is consistent with Prigogine's formulation. Here, dS or S denotes the total entropy, while Δe_p or d_iS indicates the internal entropy production. The entropy extraction is represented as d_eS or Δh_d.

The dependence of entropy on the model parameter can be explored via Eq. (9). As shown in Figure 4, the entropy of the system exhibits an intriguing parameter dependence. For $t \neq 0$, $S > 0$ which indicates that in the presence of symmetry-breaking fields such as nonuniform temperature or external force, the system is driven out of equilibrium. $S(t)$ is also considerably larger when four ratchet potentials are arranged ($M = 4$) in the network. The entropy decreases as the number of ratchet potentials (M) decreases which is reasonable since the entropy of the system depends on the number of acceptable states (lattices).

In the absence of load and at a steady state, the entropy approaches

$$
\begin{aligned}
S = &-\xi\left(e^{E/T_h}\left(1+2e^{E/T_c}\right) ln\left[\frac{e^{E/T_h}\left(1+2e^{E/T_c}\right)}{\left(1+e^{E/T_c}+e^{\frac{2E}{T_c}}\right)\left(1+2e^{E/T_h}\right)}\right]\right)\\
&+\xi\left(\left(1+e^{E/T_c}+e^{E/T_h}\right) ln\left[\frac{1+e^{E/T_c}+e^{E/T_h}}{\left(1+e^{E/T_c}+e^{\frac{2E}{T_c}}\right)\left(1+2e^{E/T_h}\right)}\right]\right)\\
&-\xi\left(e^{\frac{2E}{T_c}}\left(1+2e^{E/T_h}\right) ln\left[\frac{e^{E/T_c}}{1+2Cosh\left[\frac{E}{T_c}\right]}\right]\right),
\end{aligned}
\tag{25}
$$

$$
\begin{aligned}
S = &-\xi\left(\left(e^{E/T_h}\left(1+2e^{E/T_c}\right)\right)\left(\frac{E}{T_h}+ln\left[1+2e^{E/T_c}\right]-ln\left[2\left(1+e^{E/T_c}+e^{\frac{2E}{T_c}}\right)\left(1+2e^{E/T_h}\right)\right]\right)\right)\\
&+\xi\left(\left(1+e^{E/T_c}+e^{E/T_h}\right) ln\left[\frac{2\left(1+e^{E/T_c}+e^{\frac{2E}{T_c}}\right)\left(1+2e^{E/T_h}\right)}{1+e^{E/T_c}+e^{E/T_h}}\right]\right)\\
&-\xi\left(e^{\frac{2E}{T_c}}\left(1+2e^{E/T_h}\right) ln\left[\frac{e^{E/T_c}}{1+2Cosh\left[\frac{E}{T_c}\right]}\right]\right),
\end{aligned}
\tag{26}
$$

and

$$S = -\xi\left(e^{E/T_h}\left(1+2e^{E/T_c}\right)\left(\frac{E}{T_h}+ln\left[1+2e^{E/T_c}\right]-ln\left[4\left(1+e^{E/T_c}+e^{\frac{2E}{T_c}}\right)\left(1+2e^{E/T_h}\right)\right]\right)\right)$$

$$+\xi\left(\left(1+e^{E/T_c}+e^{E/T_h}\right)ln\left[\frac{4\left(1+e^{E/T_c}+e^{\frac{2E}{T_c}}\right)\left(1+2e^{E/T_h}\right)}{1+e^{E/T_c}+e^{E/T_h}}\right]\right)$$

$$-\xi\left(e^{\frac{2E}{T_c}}\left(1+2e^{E/T_h}\right)ln\left[\frac{e^{E/T_c}}{1+2Cosh\left[\frac{E}{T_c}\right]}\right]\right) \tag{27}$$

for $M=1$, $M=2$ and $M=4$, respectively. Here $\xi = \dfrac{1}{\left(1+e^{E/T_c}+e^{\frac{2E}{T_c}}\right)\left(1+2e^{E/T_h}\right)}$.

Taylor expanding Eqs. (25), (26), and (27) near $E=0$ leads to

$$S = ln[3] + \frac{\left(-T_c^2 - T_cT_h - 7T_h^2\right)E^2}{27T_c^2T_h^2}, \tag{28}$$

$$S = \frac{1}{3}(2ln[2]+3ln[3]) - \frac{ln[2]E}{3T_c} + \frac{\left(-2T_c^2 - 2T_cT_h - 14T_h^2 - 3T_h^2ln[2]\right)E^2}{54T_c^2T_h^2} \tag{29}$$

and

$$S = \frac{1}{3}(4ln[2]+3ln[3]) - \frac{2ln[2]E}{3T_c} + \frac{\left(-T_c^2 - T_cT_h - 7T_h^2 - 3T_h^2ln[2]\right)E^2}{27T_c^2T_h^2}. \tag{30}$$

At equilibrium, when $E \to 0$, Eqs. (28), (29), and (30) converge to $S = ln[3]$, $S \approx ln[5]$ and $S \approx ln[9]$ which reasonable since S relies on the lattice size. The system can be driven out of equilibrium as long as it operates at a finite time even in the absence of potential and load. This can be appreciated by analyzing the general time-dependent entropy S in the limit $f \to 0$, $T_h \to T_c$, and $E \to 0$. Near $t=0$, we get $S = (1+ln[2]-ln[t])t$ for all M and in the limit $t \to \infty$, we recover $S = ln[3]$, $S \approx ln[5]$ and $S \approx ln[9]$ for $M=1$, $M=2$ and $M=4$, respectively.

Entropy production and extraction rates.-In this section, the dependence for the rate of entropy production $\dot{e}_p(t)$, rate of entropy $\dot{S}(t)$, and rate of entropy extraction $\dot{h}_d(t)$ on the system parameters will be explored. Via Eqs. (13), (14), and (15), the expression for $\dot{S}(t)$, $\dot{h}_d(t)$ and $\dot{e}_p(t)$ can be evaluated. Figure 5 shows the plot of $\dot{S}(t)$ as a function of function of t, τ and M. As depicted by the figure, the rate of entropy $\dot{S}(t)$ is higher for larger lattice size M. Figure 6 shows the plot of $\dot{e}_p(t)$ as a function of t, τ and M. $\dot{e}_p(t)$ significantly large when M is large. The plot of $\dot{h}_d(t)$ as a function of t, τ, and M is exhibited in Figure 7. The figure shows that $\dot{h}_d(t)$ significantly becomes large as the network size steps up. The three figures also indicate that $\dot{e}_p(t)$ and $\dot{h}_d(t)$ approach their steady state values $\dot{e}_p = \dot{h}_d$ as time progresses. Our analysis also confirms that in the presence of symmetry-breaking fields, the entropy production rate $\dot{e}_p$ steps down in time and at steady state, $\dot{e}_p = \dot{h}_d > 0$. However, for an isothermal case and in the absence of load, $\dot{e}_p = \dot{h}_d = 0$ in a long time limit.

For any M, at steady state we find

$$\dot{e}_p(t)=\dot{h}_d(t)=-\frac{\left(e^{E/T_c}-e^{\frac{2f}{T_c}+\frac{E+f}{T_h}}\right)\left(\begin{array}{l}\ln\left[\frac{e^{E/T_c}+e^{\frac{2f}{T_c}}+e^{\frac{2f}{T_c}+\frac{E+f}{T_h}}}{2e^{E/T_c}+e^{\frac{2f}{T_c}}}\right]\\ -\ln\left[\frac{e^{E/T_c}\left(2+e^{-\frac{E+f}{T_h}}\right)}{2e^{E/T_c}+e^{\frac{2f}{T_c}}}\right]-\ln\left[\frac{1+e^{\frac{E-2f}{T_c}}+e^{\frac{E+f}{T_h}}}{1+2e^{\frac{E+f}{T_h}}}\right]\end{array}\right)}{2\left(e^{E/T_c}+e^{\frac{2f}{T_c}}+e^{\frac{2E+f}{T_c}}\right)\left(1+2e^{\frac{E+f}{T_h}}\right)}. \tag{31}$$

Analyzing the entropy production is not only vital in describing non-equilibrium systems but also signifies the degree of irreversibility of a given system. As indicated by Eq. (31), $\dot{e}_p(t)=\dot{h}_d(t)>0$ as long as $f\neq 0$ and when a distinct temperature between the hot and cold bath is retained $T_h\neq T_c$. At stall force (in the limit $f\to f^s$), $\dot{e}_p(t)=\dot{h}_d(t)=0$. The phase space at which the entropy production rate becomes zero is depicted in Figure 8.

In the absence of load f, potential E, and in the limit $T_h\to T_c$, the system relaxes to its equilibrium state in the long time limit. On the contrary, in the short time limit, the system still operates irreversibly. This can be appricated by analyzing $\dot{S}(t)$, $\dot{h}_d(t)$ and $\dot{e}_p(t)$ in the absence of load f, potential E, and in the limit $T_h\to T_c$. For $M=1$ case, one finds $\dot{h}_d(t)=0$ and

$$\dot{e}_p(t)=\dot{S}(t)=-e^{\frac{-3t}{2}}\ln\left[\frac{-1+e^{\frac{3t}{2}}}{2+e^{\frac{3t}{2}}}\right]. \tag{32}$$

On the other hand, for $M=2$ case, we get

$$\begin{aligned}\dot{e}_p(t)=&\frac{1}{8}e^{-3t/2}\left(-\left(-1+e^t\right)\ln\left[-\frac{1+e^{t/2}-2e^t}{2\left(1+e^{t/2}+e^t\right)}\right]+\left(-1+e^t\right)\ln\left[\frac{2\left(1+e^{t/2}+e^t\right)}{-1-e^{t/2}+2e^t}\right]\right.\\&-\ln\left[\frac{5+5e^{t/2}+2e^t}{2\left(1+e^{t/2}+e^t\right)}\right]+e^t\ln\left[\frac{5+5e^{t/2}+2e^t}{2\left(1+e^{t/2}+e^t\right)}\right]-4\ln\left[-5+3e^t+2e^{3t/2}\right]\\&\left.-\ln\left[\frac{2\left(-1+e^{3t/2}\right)}{7+3e^t+2e^{3t/2}}\right]-e^t\ln\left[\frac{2\left(-1+e^{3t/2}\right)}{7+3e^t+2e^{3t/2}}\right]+4\ln\left[7+3e^t+2e^{3t/2}\right]\right)\end{aligned} \tag{33}$$

$$\begin{aligned}\dot{S}(t)=&\frac{1}{8}e^{-3t/2}\left(-\left(-1+e^t\right)\ln\left[-\frac{1+e^{t/2}-2e^t}{4\left(1+e^{t/2}+e^t\right)}\right]+\left(-1+e^t\right)\ln\left[\frac{4\left(1+e^{t/2}+e^t\right)}{-1-e^{t/2}+2e^t}\right]\right.\\&-\ln\left[\frac{5+5e^{t/2}+2e^t}{4\left(1+e^{t/2}+e^t\right)}\right]+e^t\ln\left[\frac{5+5e^{t/2}+2e^t}{4\left(1+e^{t/2}+e^t\right)}\right]-4\ln\left[-5+3e^t+2e^{3t/2}\right]\end{aligned}$$

$$-3\ln\left[\frac{4\left(-1+e^{3t/2}\right)}{7+3e^{t}+2e^{3t/2}}\right]-e^{t}\ln\left[\frac{4\left(-1+e^{3t/2}\right)}{7+3e^{t}+2e^{3t/2}}\right]+4\ln\left[7+3e^{t}+2e^{3t/2}\right]\Bigg) \tag{34}$$

$$\dot{h}_d(t)=\frac{1}{2}e^{-3t/2}\ln[2]. \tag{35}$$

Once again in a quasistatic limit, regardless of any parameter choice, we find $\dot{e}_p=\dot{h}_d(t)=0$. As pointed out by Ge et al. [41], the vanishing of velocity may not indicate the system is at thermodynamic equilibrium

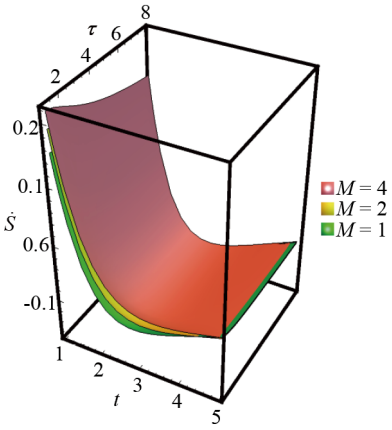

Figure 5. (Color online) $\dot{S}(t)$ versus t is evaluated analytically for fixed $\varepsilon=2.0$, $\tau=2.0$ and $\lambda=0.6$. In the figure, M is fixed as $M=4$, $M=2$, and $M=1$ from top to bottom respectively. As shown in the figure, $\dot{S}(t)$ decreases as M and t increase. At a steady state, all of these thermodynamic quantities approach the same value

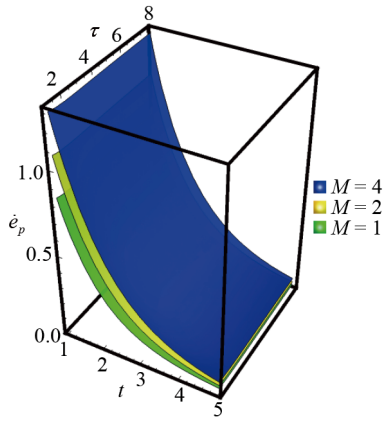

Figure 6. (Color online) The entropy production rate $\dot{e}_p(t)$ as a function of t for fixed $\varepsilon=2.0$, $\tau=2.0$ and $\lambda=0.6$. M is fixed as $M=4$, $M=2$ and $M=1$ from top to bottom, respectively. As shown in the figure, $\dot{e}_p(t)$ decreases as M and t increase. At a steady state, all of these thermodynamic quantities approach the same value

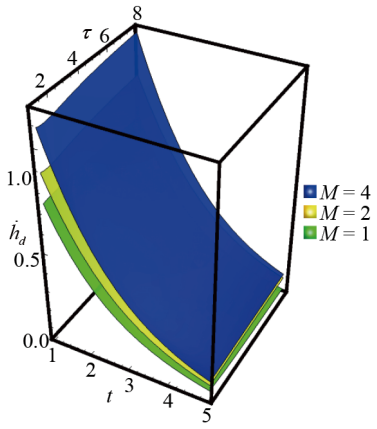

Figure 7. (Color online) The entropy extraction rate $\dot{h}_d(t)$ as a function of t evaluated analytically using Eq. (3) for a given value of $\varepsilon = 2.0$, $\tau = 2.0$, $\lambda = 0.6$. In the figure, M is fixed as $M = 4$, $M = 2$, and $M = 1$ from top to bottom respectively. As shown in the figure, $\dot{S}(t)$, $\dot{h}_d(t)$ and $\dot{e}_p(t)$ decrease as M and t increase. At a steady state, all of these thermodynamic quantities approach the same value

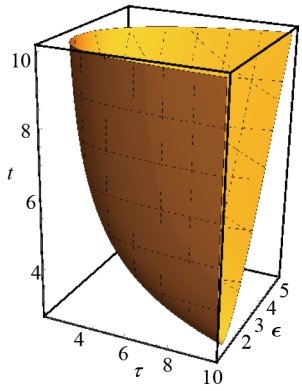

Figure 8. (Color online) (a) The Phase space at which the entropy production rate becomes zero for fixed $\lambda = 0.6$

The the analytic expressions for the change in entropy production, heat dissipation, and total entropy can be found analytically via $\Delta h_d(t) = \int_{t_0}^{t} \left(\dot{h}_d(t)\right) dt$, $\Delta e_p(t) = \int_{t_0}^{t} \left(\dot{e}_p(t)\right) dt$ and $\Delta S(t) = \int_{t_0}^{t} \left(\dot{S}(t)\right) dt$ where $\Delta S(t) = \Delta e_p(t) - \Delta h_d(t)$ and the indexes $i = 1, \ldots, 3$ and $j = 1, \ldots, 3$.

Unlike the entropy production and extraction rates, the thermodynamic relationship such as $\Delta S(t)$, $\Delta e_p(t)$ and $\Delta h_d(t)$ depend on network size even at steady state. The expressions for $\Delta h_d(t)$, $\Delta S(t)$, and $\Delta e_p(t)$ are lengthy and will not be presented in this work. As shown in Figure 9a and 9b, for a system that operates between hot and cold reservoirs, $\Delta e_p(t)$ and $\Delta h_d(t)$ approach a non-equilibrium steady state in the long time limit. As the number of lattice size steps up, $\Delta e_p(t)$ and $\Delta h_d(t)$ increase showing for large M the system exhibits a higher level of irreversibility.

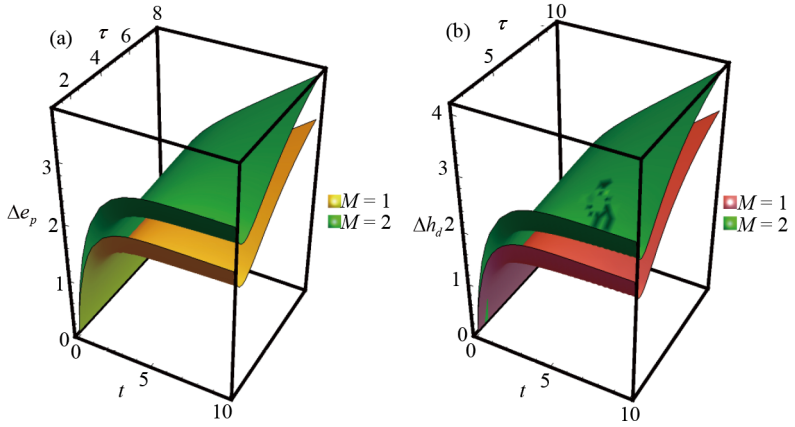

Figure 9. (Color online) (a) $\Delta e_p(t)$ as a function of t and $\tau = 2.0$ for fixed $\varepsilon = 2.0$ and $\lambda = 0.0$; (b) $\Delta h_d(t)$ as a function of t and $\tau = 2.0$ for fixed $\varepsilon = 2.0$ and $\lambda = 0.0$. In the figures, M is fixed as $M = 4$ and $M = 1$ from top to bottom respectively. As shown in the figures, $\Delta e_p(t)$ and $\Delta h_d(t)$ increase as M steps up and when t increases

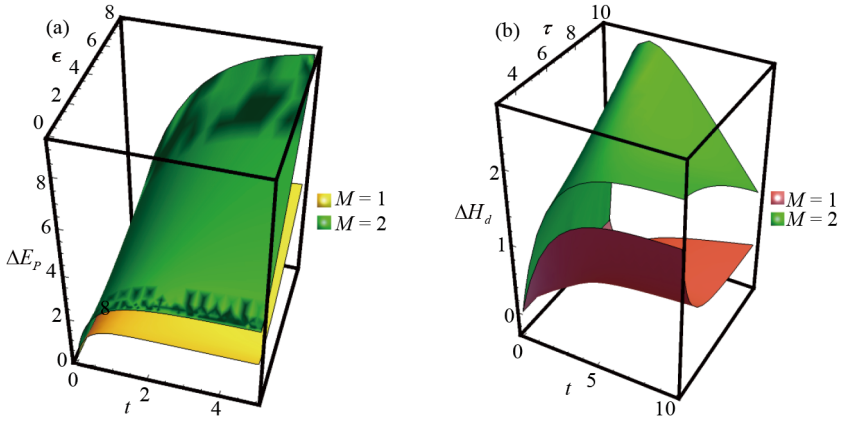

Figure 10. (Color online) (a) $\Delta E_p(t)$ as a function of t and ε for fixed $\tau = 2.0$ and $\lambda = 0$; (b) $\Delta H_d(t)$ as a function of t and τ for fixed $\varepsilon = 2.0$ and $\lambda = 0.6$. In the figures, M is fixed as $M = 2$ and $M = 1$ from top to bottom respectively. As shown in the figures, $\Delta E_p(t)$ and $\Delta H_d(t)$ increase as M steps up and when t increases

The second law of thermodynamics can be also written as $\Delta S^T(t) = \Delta E_p(t) - \Delta H_d(t)$ where $\Delta S^T(t)$, $\Delta E_p(t)$ and $\Delta H_d(t)$ are very lengthy expressions which can be evaluated via $\Delta H_d = \int_{t_0}^{t} \left(\dot{H}_d(t)\right) dt$, $\Delta E_p(t) = \int_{t_0}^{t} \left(\dot{E}_p(t)\right) dt$ and $\Delta S^T(t) = \int_{t_0}^{t} (\dot{S}^T(t)) dt$.

As discussed before, once the expressions for $\dot{H}_d(t), \dot{E}_p, \dot{S}^T$ are analyzed, the corresponding entropy balance equation can be calculated as $\frac{dS^T(t)}{dt} = \dot{E}_p - \dot{H}_d$. The expressions for these relations are very complicated. In Figure 10a we plot $\Delta E_p(t)$ as a function of t and ε for fixed $\tau = 2.0$ and $\lambda = 0$. Figure 10b depicts the plot of $\Delta H_d(t)$ as a function of t and τ for fixed $\varepsilon = 2.0$ and $\lambda = 0.6$. In both figures, M is fixed as $M = 2$ and $M = 1$ from top to bottom respectively. As shown in the same figures, $\Delta E_p(t)$ and $\Delta H_d(t)$ increase as M and t increase.

The free energy.-Next, we explore the dependence of the free energy dissipation rate shown in Eqs. (12) and (13) on t. In general $\dot{F} < 0$ and approaches zero in the long time limit for both cases (see Figure 11). As depicted in Figure 11, when the system operates at finite time, the free energy dissipation rate increases as the number of ratchet potentials M steps up. At a steady state, the free energy rate approaches the same value for all M. This can be appreciated by evaluating the rate in the long limit. At a steady state, for all M, the free energy rate converges to

$$\dot{F} = \frac{\xi\left(3f - T_h ln\left[\frac{e^{E/T_c} + e^{\frac{2f}{T_c}} + e^{\frac{2f}{T_c}+\frac{E}{T_h}+\frac{f}{T_h}}}{2e^{E/T_c} + e^{\frac{2f}{T_c}}}\right] + T_c ln\left[\frac{e^{E/T_c}\left(2 + e^{-\frac{E+f}{T_h}}\right)}{2e^{E/T_c} + e^{\frac{2f}{T_c}}}\right] + T_c ln\left[\frac{1 + e^{\frac{E-2f}{T_c}} + e^{\frac{E+f}{T_h}}}{1 + 2e^{\frac{E+f}{T_h}}}\right]\right)}{2\xi\left(1 + 2e^{\frac{E+f}{T_h}}\right)} \tag{36}$$

where $\xi = \left(-e^{E/T_c} + e^{\frac{2f}{T_c}+\frac{E}{T_h}+\frac{f}{T_h}}\right)$. For the isothermal case, in the absence of potential barrier and load, Eq. (37) approaches zero since the detail balance condition is fulfilled. Moreover $\Delta U = \Delta H_d = 0$ and $\Delta F(t) = -\Delta E_p$. At equilibrium ($t \to \infty$), we get $\Delta F = -T_c \ln(3)$ for $M = 1$.

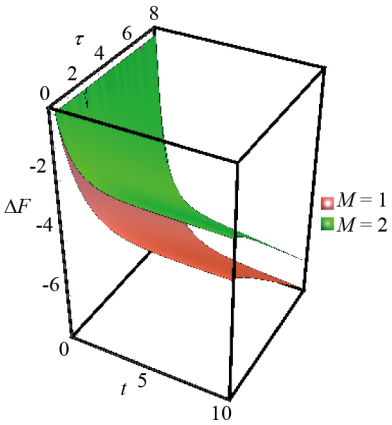

Figure 11. (Color online) (a) The change in free energy ΔF versus t and τ for $f = 0.0$ and $\varepsilon = 2.0$. In the figure, $M = 1$ and $M = 2$ from the top to bottom

When the system operates at a finite time, the system operates irreversibly, in the absence of potential barrier and load. Taylor expanding the free energy rate near $t = 0$, one gets $\dot{F} = -T_c(ln[2] - ln[t])$ for $M = 1$ and $\dot{F} = -1/8T_c(15ln[2] - ln[8] - lnLog[t])$ for $M = 2$ case. The change in free energy ΔF versus t and τ is depicted in Fig. 11 for fixed $f = 0.0$ and $\varepsilon = 2.0$. In the figure, $M = 1$ and $M = 2$ from the top to bottom. from the top to bottom.

2.3 *Heat transfer via kinetic energy*

So far, the rate of heat loss due to particle recrossing at the boundary between the hot and cold reservoirs is not included. When the heat exchange via kinetic energy is included, the system becomes irreversible even at the quasistatic limit, and as a result $\dot{e}_p \neq 0$ or $\dot{E}_p \neq 0$.

During the biased random walk, the particle absorbs $k_B(T_h - T_c)/2$ amount of heat from the hot bath. It then gives back $k_B(T_h - T_c)/2$ amount of heat to the cold bath. As a result, there will be an irreversible heat flow from the hot to cold baths. The rate of heat transfer from the hot to the cold reservoirs $\dot{Q}_{irr}(t)$ depends on how often the particle jumps from the cold to the hot heat baths. After some algebra, one gets

$$\dot{Q}_{irr}(t) = (p_1 P_{21} + p_3 P_{23})(T_h - T_c)/2 \tag{37}$$

for $M = 1$ case and

$$\dot{Q}_{irr}(t) = (p_1 P_{21} + p_3 P_{23})(T_h - T_c)/2 +$$

$$\left(p_1 P'_{21} + p'_3 P'_{23}\right)(T_h - T_c)/2 \tag{38}$$

for $M = 2$ case. At steady state, for all M we find

$$\dot{Q}_{irr} = -\frac{\left(2e^{E/T_c} + e^{\frac{2f}{T_c}}\right)\left(1 + e^{\frac{E+f}{T_h}}\right)(T_c - T_h)}{4\left(e^{E/T_c} + e^{\frac{2f}{T_c}} + e^{\frac{2E+f}{T_c}}\right)\left(1 + 2e^{\frac{E+f}{T_h}}\right)}. \tag{39}$$

For the case where $f = 0$ and $E = 0$, one gets

$$\dot{Q}_{irr}(t) = -\frac{1}{6}e^{-3t/2}\left(2 + e^{3t/2}\right)(T_c - T_h). \tag{40}$$

Integrating Eq. (41) with respect to time yields

$$\Delta Q_{irr}(t) = -\frac{1}{18}e^{-3t/2}\left(-4 + e^{3t/2}(4 + 3t)\right)(T_c - T_h) \tag{41}$$

as long as $f = 0$ and $E = 0$.

One can note that the heat transfer through the kinetic energy does not affect $\dot{H}_d$ as the heat taken from the hot reservoirs goes to the cold reservoir. This also implies that the whole heat dumped to the cold reservoirs contributes to the internal entropy production and hence for any parameter choice $\dot{E}_p(t) > 0$ as long as $T_h \neq T_c$. The heat loss due to particle recrossing contributes to the internal entropy production and we infer the new entropy production rate to be

$$\dot{E}^*_p(t) = \dot{E}_p(t) + \dot{Q}_{irr}(t). \tag{42}$$

One can then rewrite the thermodynamic relations derived in the previous section in terms of $\dot{E}^*_p(t)$. Here $\dot{E}^*_p = 0$ only when $T_h = T_c$.

The rate of free energy depicted in Eq. (19), can be rewritten as

$$\dot{F}(t) + \dot{E}_p(t) + \dot{Q}_{irr}(t) = \dot{U}(t) + \dot{H}_d(t) = -fV(t) \tag{43}$$

The change in the free energy is given by

$$\Delta F(t) = -\int_{t_0}^{t} \left(fV(t) + \dot{E}_p(t) + \dot{Q}_{irr}(t)\right) dt$$

$$= \int_{t_0}^{t} \left(\dot{U}(t) + \dot{H}_d(t) - \dot{E}_p(t) + \dot{Q}_{irr}(t)\right) dt$$

$$= \Delta U + \Delta H_d - \Delta E_p - \Delta Q_{irr}(t). \tag{44}$$

In the absence of load and potential energy, for all M at steady state, Eq. (44) converges to

$$\dot{E}_p^* = -\dot{F}(t) = \dot{Q}_{irr}(t) = \frac{1}{6}(-T_c + T_h). \tag{45}$$

Eq. (46) confirms the second law of thermodynamics in essence that the entropy for a thermally driven heat engine is greater than zero. In other words, such systems operate irreversibly as long as a distinct temperature difference is retained between the hot and cold heat baths. For isothermal cases $T_h \to T_c$, $\dot{Q}_{irr}(t) \to 0$ as expected. Eq. (46) also reconfirms Clausius' statement of the second law [1] that "Heat can never pass from a colder to a warmer body without some other change, connected therewith, occurring at the same time." In the next section, using complex generating functions, we show the rate for thermodynamic relations does not depend on the network size M at steady state.

2.4 *Alternative derivation of velocity via complex generating functions*

In this section, we show why the rate for thermodynamic relations does not depend on the network size M at steady state, the mathematical approach discussed by Goldhirsch et al. [42, 43] is adapted. Using this mathematical approach, we also calculated the velocity of the motor in our recent paper [44].

For clarity, first, we revise the mathematical technique developed. Consider a segment with sites 0, 1 ,2, ..., N as shown in Figure 1b. Let $P_{2,1}$ be the probability per unit time step for the walker to jump from 1 to 2 while $P_{1,2}$ be the probability to jump from 2 to 1 with a condition $P_{1,2} + P_{2,1} \leq 1$. The probability $P_w(n)^+$ designates the probability for the walker to start at $j = 0$ and reach $j = N$ in n steps in the right direction. The mean first passage for the walker to reach $j = N$ for the first time is given as [44]

$$\left\langle t^+ \right\rangle = \frac{\sum_{n=0}^{n=\infty} nP_w(n)^+}{\sum_{n=0}^{n=\infty} P_w(n)^+}. \tag{46}$$

The corresponding generating function in terms of the ϕ probability for $P_w(n)^+$ is given by

$$G_N(\phi)^+ = \sum_{n=0}^{n=\infty} e^{i\phi n} P_w(n)^+ \tag{47}$$

where in this case $0 < \phi < 2\pi$. In terms of generating function, the corresponding mean first passage time shown in Eq. (46) can be written as

$$t^{+}=\frac{\frac{d}{d(i\phi)}G_N(\phi)^{+}}{G_N(\phi)^{+}}|_{\phi=0}=\frac{d}{d(i\phi)}G_N(\phi)^{+}|_{\phi=0}. \tag{48}$$

$P_1,\ P_2,\ ...$, are given by $P_1e^{i\phi},\ P_2e^{i\phi},\ ...$, in terms of ϕ probabilities. The particle has a probability $(1-P_1)^n$ to stay at $j=0$ after n consecutive steps. The corresponding generating function is written as

$$X_{1-P_{1,2}}=\sum_{n=0}^{n=\infty}(1-P_{1,2})^n e^{i\phi n}$$

$$=\frac{1}{1-(1-P_1)e^{i\phi}}. \tag{49}$$

Similarly, in terms of generating function, the probability of staying at site j after n consecutive steps is given by

$$X_{1-P_{1,\ 2}-P_{2,\ 1}}=\sum_{n=0}^{n=\infty}(1-P_{1,\ 2}-P_{2,\ 1})^n e^{i\phi n}$$

$$=\frac{1}{1-(1-P_{1,\ 2}-P_{2,\ 1})e^{i\phi}}. \tag{50}$$

Let us $U(n)^{+}$ to be the probability for the walker to leave $j=0$ and reaches $j=N$ in the right direction without returning to $j=0$. The associated generating function can be expressed as

$$T_N^{+}=\sum_{n=0}^{n=\infty}e^{i\phi n}U(n)^{+}. \tag{51}$$

Similarly, let $V(n)^{+}$ be the probability for the walker to leave $j=0$ in the right direction and returns to $j=0$ without reaching $j=N$. The corresponding generating function is given by

$$Q_N(\phi)^{+}=\sum_{n=0}^{n=\infty}e^{i\phi n}V(n)^{+}. \tag{52}$$

To reach the point $j=N$, the particle can stay at the site $j=0$ for a number of steps with probability $X_{1-P_{1,\ 2}}$, moves out, and returns to $j=0$ without touching $j=N$ with Q_N^{+} probability then stay at $j=0$. These recursive steps are repeated many times as shown below

$$R_1^{+}=X_{1-P_{1,\ 2}}+X_{1-P_{1,\ 2}}Q_N^{+}X_{1-P_{1,\ 2}}+X_{1-P_{1,\ 2}}Q_N^{+}X_{1-P_{1,\ 2}}Q_N^{+}X_{1-P_{1,\ 2}}+...$$

$$=\frac{X_{1-P_{1,\ 2}}}{1-Q_N^{+}X_{1-P_{1,\ 2}}}. \tag{53}$$

The particle finally will reach the site $j = N$ without returning to $j = 0$ with the ϕ probability of T_N^+ after several trials. Thus the generating function $G_N(\phi)^+$ for the first passage time takes a form

$$G_N(\phi)^+ = R_1^+ T_N^+ = \frac{X_{1-P_{1,\,2}} T_N^+}{1 - X_{1-P_{1,\,2}} Q_N^+(\phi)} \tag{54}$$

For the Brownian particle moving in complex networks, let us now calculate the generating function for the MFPT in the right direction (see Figure 2a). To reach the other side of the potential well, the particle can stay at the site where the hot bath is located for a number of steps with probability $X'_{1-P_{1,\,2}}$, moves out and returns to the hot bath using one of the M possible paths with ϕ probability $(Q_1^+ + ... + Q_M^+)$. The particle then stays in the hot bath. The particle repeats these recursive steps many times as shown below

$$\begin{aligned} R_1^+ =& X'_{1-P_1} + X'_{1-P_{1,\,2}}(Q_1^+ + ... + Q_M^+) X'_{1-P_{1,\,2}} + X'_{1-P_{1,\,2}}(Q_1^+ + ... + Q_M^+) X'_{1-P_{1,\,2}}(Q_1^+ + ... + Q_M^+) X'_{1-P_1} + ... \\ =& \frac{X'_{1-P_{1,\,2}}}{1 - (Q_1^+ + ... + Q_M^+) X'_{1-P_{1,\,2}}} \end{aligned} \tag{55}$$

where $Q_j^+ = P_{1,\,2} e^{i\phi} P_{2,\,1} e^{i\phi}$, $\{j = 1,\ ...,\ M\}$is defined as the ϕ probability for the walker to leave the hot bath and returns back to the hot bath without touching the other side of the potential well. After several trials, the particle finally will be able to reach the other side of the potential without returning to the hot bath using one of the possible M paths with ϕ probability $(T_1^+ + ... + T_M^+)$. Here $T_j^+ = P_{1,\,2} e^{i\phi} P_{3,\,1} e^{i\phi}$, $\{j = 1,\ ...,\ M\}$ is the ϕ probability (for the j^{th} ratchet potential) for the walker to leave the hot bath and reach the other side of the potential well in the right direction without returning to the hot bath. The generating function for the MFPT towards the right direction is given by

$$\begin{aligned} G_M(\phi)^+ =& R_1^+ (T_1^+ + ... + T_M^+) \\ =& \frac{X'_{1-P_1}(T_1^+ + ... + T_M^+)}{1 - X'_{1-P_1}(Q_1^+ + ... + Q_M^+)}. \end{aligned} \tag{56}$$

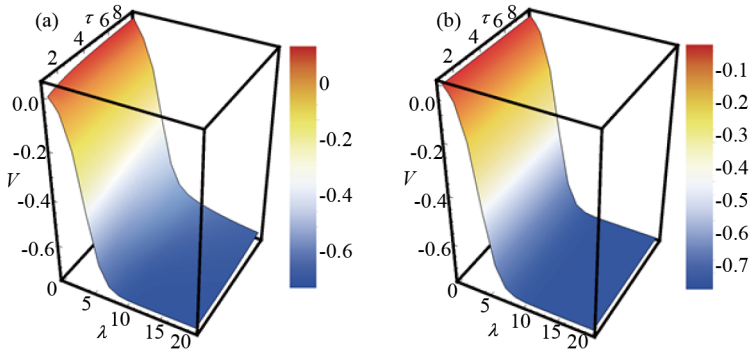

Figure 12. (Color online) (a) Particle velocity V as a function of τ and λ is plotted via Eq. (21) for fixed $\varepsilon = 2.0$; (b) Particle velocity V as a function of τ and λ is plotted via Eq. (59) for fixed $\varepsilon = 2.0$

Following the above steps, the generating function for the MFPT to the left direction can be also given as

$$G_M(\phi)^- = \frac{X'_{1-P_{3,1}}(T_1^- + ... + T_M^-)}{1 - X'_{1-P_{3,1}}(Q_1^- + ... + Q_M^-)} \tag{57}$$

where $T_j^- = P_{3,\,1}e^{i\phi}P_2e^{i\phi},\ \{j = 1,\ ...,\ M\}$is the ϕ probability (for the j^{th} ratchet potential) for the walker to leave the cold bath (left potential well) and to reach the other side of the potential well in the left direction without returning to the cold bath while $Q_j^- = P_4e^{i\phi}P_3e^{i\phi},\ \{j = 1,\ ...,\ M\}$is defined as the ϕ probability for the walker to leave the cold bath (towards the left direction) and return to the cold bath without touching the other side of the potential well. For clarity let us write $X'_{1-P_{1,\,2}} = \frac{1}{1-(1-MP_{1,\,2})e^{i\phi}}$and $X'_{1-P_{3,\,1}} = \frac{1}{1-(1-MP_{3,\,1})e^{i\phi}}$. Care must be taken that now $P_{1,\,2} = \frac{1}{M}e^{-(E+df)/T_h}$, $P_{2,\,1} = \frac{1}{2}$, $P_{3,\,1} = \frac{1}{2}$ and $P_{1,\,3} = \frac{1}{M}e^{-(E-df)/T_c}$. Since we have M identical potentials, the net average velocity (independent of lattice size M) is simplified to

$$\begin{aligned} V =& (V^+ - V^-) \\ =& 3\frac{e^{\frac{2E}{T_c}} + e^{f/T_c} - e^{\frac{f}{T_c}+\frac{E+f}{T_h}}\left(1 + e^{\frac{E+f}{T_c}}\right)}{2\left(e^{\frac{2E}{T_c}} + e^{f/T_c}\right)\left(1 + e^{\frac{E+f}{T_c}}\right)\left(1 + 2e^{\frac{E+f}{T_h}}\right)} \end{aligned} \tag{58}$$

The approximated velocity in Eq. (59) is approximately the same as the velocity shown in Eq. (21). This can be appreciated by plotting V as a function of time t in Figure 12a and 12b.

3. Brownian particle operating in a heat bath where its temperature linearly decreases along with the reaction coordinate

Let us now consider M ratchet potentials arranged in a lattice (see Figure 13) where each ratchet potential is coupled with a linearly decreasing temperature

$$T_i = T_h + \frac{(i-1)(T_c - T_h)}{3} \tag{59}$$

as shown in Figure 14. Once again, the rate equation for the model is given by $\frac{d\vec{p}}{dt} = \mathbf{P}\vec{p}$ where the expression for $\mathbf{P}$ can be evaluated for any M. For instance, for a single ratchet potential $M = 1$, $\mathbf{P}$ is a 3 by 3 matrix which is given by

$$\mathbf{P} = \begin{pmatrix} \frac{-\mu_1 a_1}{2} - \frac{\mu_2^2}{2a_2} & \frac{1}{2} & \frac{1}{2} \\ \frac{\mu_1 a_1}{2} & \frac{-1-\nu b}{2} & \frac{1}{2} \\ \frac{\mu_2^2}{2a_2} & \frac{\nu b}{2} & -1 \end{pmatrix}. \tag{60}$$

For two ratchet potentials ($M = 2$), $\mathbf{P}$ has a form

$$\mathbf{P}=\begin{pmatrix} \frac{-2\mu_1 a_1}{2}-\frac{2\mu_2^2}{2a_2} & \frac{1}{2} & \frac{1}{2} & \frac{1}{2} & \frac{1}{2} \\ \frac{\mu_1 a_1}{2} & \frac{-1-\nu b}{2} & 0 & \frac{1}{2} & 0 \\ \frac{\mu_1 a_1}{2} & 0 & \frac{-1-\nu b}{2} & 0 & \frac{1}{2} \\ \frac{\mu_2^2}{2a_2} & \frac{\nu b}{2} & 0 & -1 & 0 \\ \frac{\mu_2^2}{2a_2} & 0 & \frac{\nu b}{2} & 0 & -1 \end{pmatrix} \tag{61}$$

while for $M=3$ and $M=4$ cases, one gets

$$\mathbf{P}=\begin{pmatrix} \frac{-3\mu_1 a_1}{2}-\frac{3\mu_2^2}{2a_2} & \frac{1}{2} & \frac{1}{2} & \frac{1}{2} & \frac{1}{2} & \frac{1}{2} & \frac{1}{2} \\ \frac{\mu_1 a_1}{2} & \frac{-1-\nu b}{2} & 0 & 0 & \frac{1}{2} & 0 & 0 \\ \frac{\mu_1 a_1}{2} & 0 & \frac{-1-\nu b}{2} & 0 & 0 & \frac{1}{2} & 0 \\ \frac{\mu_1 a_1}{2} & 0 & 0 & \frac{-1-\nu b}{2} & 0 & 0 & \frac{1}{2} \\ \frac{\mu_2^2}{2a_2} & \frac{\nu b}{2} & 0 & 0 & -1 & 0 & 0 \\ \frac{\mu_2^2}{2a_2} & 0 & \frac{\nu b}{2} & 0 & 0 & -1 & 0 \\ \frac{\mu_2^2}{2a_2} & 0 & 0 & \frac{\nu b}{2} & 0 & 0 & -1 \end{pmatrix} \tag{62}$$

and

$$\mathbf{P}=\begin{pmatrix} \frac{-4\mu_1 a_1}{2}-\frac{4\mu_2^2}{2a_2} & \frac{1}{2} & \frac{1}{2} & \frac{1}{2} & \frac{1}{2} & \frac{1}{2} & \frac{1}{2} & \frac{1}{2} & \frac{1}{2} \\ \frac{\mu_1 a_1}{2} & \frac{-1-\nu b}{2} & 0 & 0 & 0 & \frac{1}{2} & 0 & 0 & 0 \\ \frac{\mu_1 a_1}{2} & 0 & \frac{-1-\nu b}{2} & 0 & 0 & 0 & \frac{1}{2} & 0 & 0 \\ \frac{\mu_1 a_1}{2} & 0 & 0 & \frac{-1-\nu b}{2} & 0 & 0 & 0 & \frac{1}{2} & 0 \\ \frac{\mu_1 a_1}{2} & 0 & 0 & 0 & \frac{-1-\nu b}{2} & 0 & 0 & 0 & \frac{1}{2} \\ \frac{\mu_2^2}{2a_2} & \frac{\nu b}{2} & 0 & 0 & 0 & -1 & 0 & 0 & 0 \\ \frac{\mu_2^2}{2a_2} & 0 & \frac{\nu b}{2} & 0 & 0 & 0 & -1 & 0 & 0 \\ \frac{\mu_2^2}{2a_2} & 0 & 0 & \frac{\nu b}{2} & 0 & 0 & 0 & -1 & 0 \\ \frac{\mu_2^2}{2a_2} & 0 & 0 & 0 & \frac{\nu b}{2} & 0 & 0 & 0 & -1 \end{pmatrix}. \tag{63}$$

Here $\mu_1=e^{-E/T_1}$, $\nu=e^{-(E+f)/T_2}$, $a_1=e^{-f/T_1}$, $\mu_2=e^{-E/T_4}$ and $a_2=e^{-f/T_4}$.

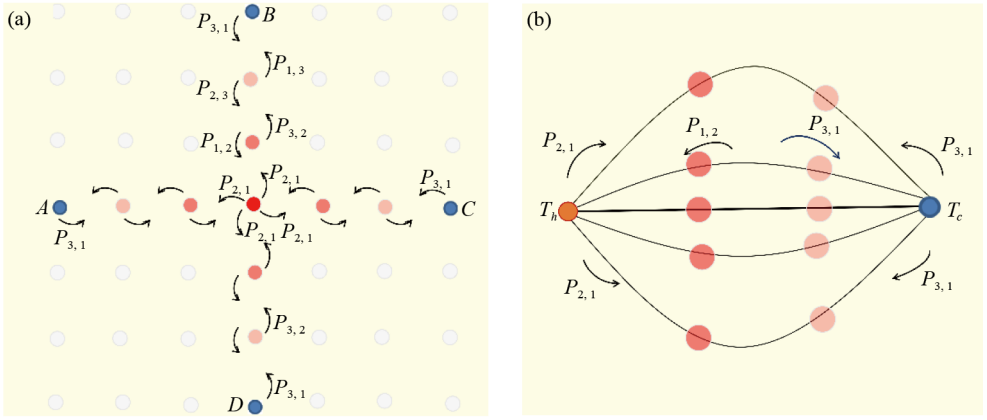

Figure 13. (Color online) (a) Four thermal ratchets are arranged in a lattice where in each ratchet potential the temperature is arranged to decrease linearly from the hotter bath (T_h) to the colder bath (T_c). The hotter bath for the four Brownian ratchets are located at the center; (b) A schematic diagram is plotted by imposing a periodic boundary condition (when one binds the nodes A, B, C, D of Figure 13a together). Figure 13a and 13b are the same (when $M = 4$)

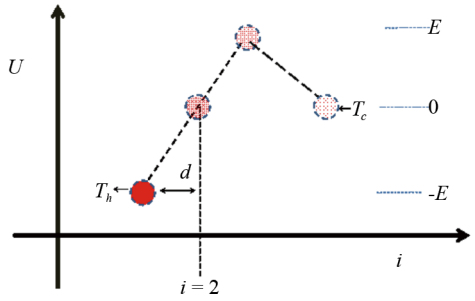

Figure 14. (Color online) The schematic diagram for a Brownian particle that walks in a discrete ratchet potential coupled with a linearly decreasing temperature heat bath. The temperature for the heat bath decreases from T_h to T_c according to Eq. (60)

Since the temperature linearly decreases, the parameter $T_1 = T_h$, $T_2 = T_h + (T_c - T_h)/3$, $T_3 = T_h + 2(T_c - T_h)/3$ and $T_4 = T_c$. The sum of each column of the matrix $\mathbf{P}$ is zero, $\sum_m \mathbf{P}_{mn} = 0$ which reveals that the total probability is conserved: $(d/dt)\sum_n p_n = d/dt(\mathbf{1}^T \cdot p) = \mathbf{1}^T \cdot (\mathbf{P}\vec{p}) = 0$. It is important to note that via the expressions $p_1(t)$, $p_2(t)$ and $p_3(t)$ that are shown in Appendix A2 and using the rates,

$$P_{21} = \frac{1}{2}e^{-(E+f)/T_1}\ P_{12} = \frac{1}{2},\ P_{32} = \frac{1}{2}e^{-(E+f)/T_2}$$

$$P_{23} = \frac{1}{2},\ P_{13} = \frac{1}{2},\ P_{31} = \frac{1}{2}e^{-(2E-f)/T_4} \tag{64}$$

the thermodynamic quantities which are under investigation can be evaluated.

Once again, the velocity $V(t)$ at any time t is the difference between the forward $V_i^+(t)$ and backward $V_i^-(t)$ velocities at each site i

$$V(t)=\sum_{i=1}^{3}(V_i^{+}(t)-V_i^{-}(t))$$

$$=(p_1P_{21}-p_2P_{12})+(p_2P_{32}-p_3P_{23})+(p_3P_{13}-p_1P_{31}). \tag{65}$$

Similar to the previous section, as the number of network sizes increases, the entropy S of the system steps up. On the other hand, the velocity V, the entropy production $\dot{e}_p(t)$ as well as entropy extraction $\dot{h}_d(t)$ rates increase with network sizes. At steady state V, $\dot{e}_p(t)$ and $\dot{h}_d(t)$ become independent of the network size. For all M, at steady the velocity converges to

$$V=\frac{3\left(e^{\frac{2E}{T_c}}-e^{\frac{ET_c(T_c+5T_h)+f\left(T_c^2+6T_cT_h+2T_h^2\right)}{T_cT_h(T_c+2T_h)}}\right)}{2\left(1+2e^{\frac{3(E+f)}{T_c+2T_h}}\right)\left(e^{\frac{2E}{T_c}}+e^{\frac{2E}{T_c}+\frac{E}{T_h}+\frac{f}{T_h}}+e^{\frac{ET_c+f(T_c+T_h)}{T_cT_h}}\right)}. \tag{66}$$

The energetics of the system that operates between the hot and cold baths are also compared and contrasted with a system that operates in a heat bath where its temperature linearly decreases along the reaction coordinate. We show that a system that operates between the hot and cold baths has significantly lower velocity but a higher efficiency in comparison with a linearly decreasing case as shown in Figure 15. In the figure the ratio of velocity for a linearly decreasing case over the velocity for two heat baths cases is plotted as a function of t and τ for a given $\varepsilon=2.0$, $M=4$ and $f=0.3$.

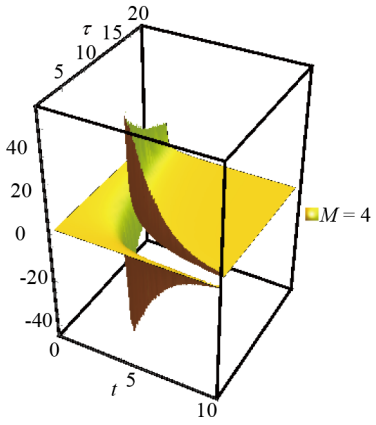

Figure 15. (Color online) The ratio of velocity for linearly decreasing case over the velocity for two heat baths case is plotted as a function of t and τ for a given $\varepsilon=2.0$ and $f=0.3$. In the figure, M is fixed as $M=4$

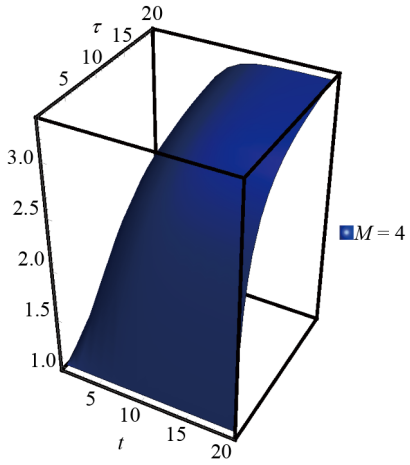

Figure 16. (Color online) The ratio of entropy for linearly decreasing case over the velocity for two heat baths case as a function of t and τ for a given $\varepsilon = 2.0$ and $f = 0.3$. In the figure, M is fixed as $M = 4$

The entropy for the linearly decreasing case is considerably larger than the entropy for two heat bath cases as shown in Figure 16.

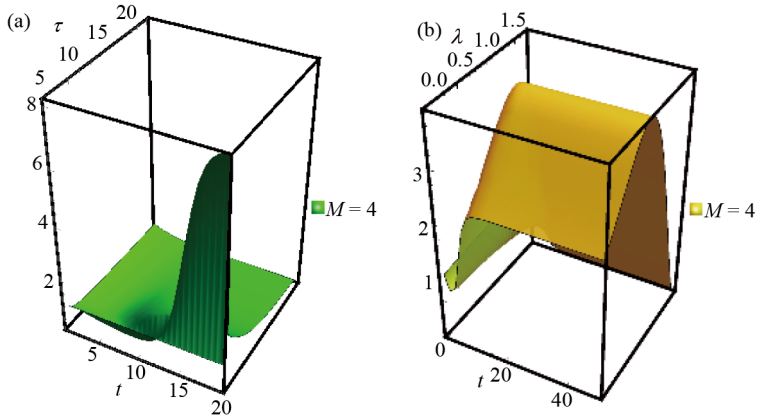

Figure 17. (Color online) (a)The ratio of entropy production rate for linearly decreasing case over the entropy production rate for two heat baths case as a function of t and τ; (b) The ratio of free energy rate for linearly decreasing case over the free energy rate for two heat baths cases as a function of t and τ. In the figures, the parameters are fixed as $M = 4$, $\varepsilon = 2.0$, and $f = 0.3$

As depicted in Figure 17a, a system that operates between the hot and cold baths has a significantly lower entropy production rate than a linearly decreasing temperature case. Moreover, in Figure 17b, we compare the ratio of the free energy rate of a linearly decreasing case with a system that operates in two heat bath cases. The figure depicts that the free energy rate is considerably large for a linearly decreasing case. Our analysis also indicates that the change in free energy becomes minimal at a steady state. However, for a system that operates in a heat bath where its temperature varies linearly in space, the change in free energy varies linearly in space.

The fact that the entropy, entropy production, and extraction rates are considerably larger for a a linearly decreasing temperature case than a Brownian particle that operates between the hot and cold baths indicates that systems exposed to a linearly decreasing temperature case are inherently irreversible and as a result, such systems have very low efficiency. On the contrary, the particle moving in a linearly decreasing thermal arrangement has a higher velocity. Thus such kind of thermal arrangement is beneficial, to designing a device that can transport a Brownian particle fast along the reaction

coordinate. A Brownian particle that operates between two heat baths has a higher efficiency but a lower velocity in comparison with a linearly decreasing temperature case. Thus such a model system is advantageous if the sole purpose is to design an efficient Brownian motor.

Experimentally, care must be taken when arranging the ratchets within the networks. As the number of Brownian ratchets increases, the interactions between them can result in complex dynamics. This complexity can lead to emergent behaviors that are difficult to predict and comprehend. The nonlinear and emergent nature of large networks of Brownian ratchets poses significant challenges for predictability and control. Understanding and managing these behaviors requires advanced modeling techniques and experimental setups capable of capturing the complicated dynamics of the system.

Experimental techniques to achieve directed motion require sophisticated setups that allow precise control over environmental conditions and the forces acting on particles. Optical tweezers, for instance, use tightly focused laser beams to manipulate particles with high precision. Realizing and controlling a network of Brownian ratchets experimentally is particularly challenging. Accurate measurement of thermodynamic variables, such as temperature, is difficult due to the small scales involved and the system's sensitivity to environmental fluctuations. Additionally, experimental setups are prone to measurement errors and noise, complicating the validation of theoretical models and simulations. In other words, environmental factors and the noise from the instruments can affect the system's experimental results and, as a result, it will be challenging to draw accurate conclusions.

4. Summary and conclusion

Most of the previous works have focused on exploring the thermodynamics feature of systems that operate in a single thermal ratchet. On the contrary, molecular motors such as kinesin, myosin, and dynein walk in microtubule networks. Most Biologically important problems such as impurities (donors) diffuse along the semiconductor layer and consequently, they require $2D$ and $3D$ analysis. Nanorobots are artificial Brownian motors and they are designed to achieve a unidirectional motion on complex networks. To address such important physical problems, an exactly solvable model is presented. The long-time, as well as the short-time behavior of the system, is explored by obtaining exact time-dependent solutions.

To comprehend the thermodynamic features of systems beyond a linear response and steady-state the regime, the thermodynamic features of a single Brownian particle that hops along M Brownian ratchets arranged in complex networks are studied. Each ratchet potential is either coupled with hot and cold reservoirs or a heat bath where its temperature decreases linearly along the reaction coordinate. Often the thermodynamic quantities such as entropy $S(t)$, entropy production $e_p(t)$, and entropy extraction $h_d(t)$ serve as an indicator of irreversibly that the system sustains. Whenever our system obeys a detail balance condition, $e_p = 0$. Conversely, when the system operates for a finite time or when it is exposed to symmetry-breaking fields, the entropy of the system may exceed zero, indicated by $e_p > 0$.

The main analytical results of this paper indicate that the rates of thermodynamic quantities such as velocity, entropy production rate, and entropy extraction rate are independent of network size at steady state. Conversely, thermodynamic relations such as entropy, entropy production, and entropy extraction increase with network size even at a steady state. The thermodynamic properties of systems operating between hot and cold baths are also compared and contrasted with those of a system operating in a heat bath where the temperature varies linearly along the reaction coordinate. Regardless of network size, the entropy, entropy production, and extraction rates are significantly larger for the linearly varying temperature case compared to systems operating between hot and cold baths, indicating that the degree of irreversibility is higher for the system that operates in a heat bath where its temperature decreases linearly along with the reaction coordinate. These results are essential for examining the thermodynamics of Brownian particles in complex networks. Protein-based molecular motors like kinesin, myosin, and dynein operate within these networks. Similarly, nanorobots, as artificial Brownian motors, achieve unidirectional motion on two-dimensional surfaces. Additionally, the diffusion of impurities in semiconductor layers requires thorough two-dimensional and three-dimensional analysis.

The exactly solvable model presented in this paper serves as a tool to explore the thermodynamic features of two-dimensional systems. When the Brownian particle is exposed to a network coupled with two heat baths, the particle

(motor) exhibits a higher efficiency but it achieves its task steadily. When the particle is exposed to a heat bath where its temperature decreases linearly, it moves faster but has lower efficiency. For all thermal arrangements, the particle attains a faster velocity whenever the network M increases. This indicates that by properly arranging the model ingredient prior to the motor operation, the motor can accomplish a specific task. Thus the exactly solvable model presented in this work not only advances the nonequilibrium statistical mechanics but also helps in designing artificial Brownian motors.

Acknowledgment

I would like to thank Hana Taye and Mulu Zebene for their constant encouragement.

Conflict of interest

This manuscript has no associated data or the data will not be deposited. Authors' comment: Since we presented an analytical work, we did not collect any data from simulations or experimental observations.

References

[1] Clausius R. On the mechanical theory of heat with application to the steam-engine. *Annals of Physics.* 1865; 201: 353.
[2] Landi GT, Paternostro M. Irreversible entropy production: from classical to quantum. *Reviews of Modern Physics.* 2021; 93: 035008.
[3] Onsager L. Reciprocal relations in irreversible processes I. *Physical Review.* 1931; 37: 405.
[4] Onsager L. Reciprocal relations in irreversible processes II. *Physical Review.* 1931; 38: 2265.
[5] Ge H, Qian H. Physical origins of entropy production, free energy dissipation, and their mathematical representations. *Physical Review E.* 2010; 81: 051133.
[6] Tome T, de Oliveira MJ. Entropy production in nonequilibrium systems at stationary states. *Physical Review Letters.* 2012; 108: 020601.
[7] Schnakenberg J. Network theory of microscopic and macroscopic behavior of master equation systems. *Reviews of Modern Physics.* 1976; 48: 571.
[8] Tome T, de Oliveira MJ. Entropy production in irreversible systems described by a Fokker-Planck equation. *Physical Review E.* 2010; 82: 021120.
[9] Zia RKP, Schmittmann B. Probability currents as principal characteristics in the statistical mechanics of nonequilibrium steady states. *Journal of Statistical Mechanics.* 2007; 2007(07): P07012.
[10] Seifert U. Entropy production along a stochastic trajectory and an integral fluctuation theorem. *Physical Review Letters.* 2005; 95: 040602.
[11] Tome T. Entropy production in nonequilibrium systems described by a Fokker-Planck equation. *Brazilian Journal of Physics.* 2006; 36: 1285.
[12] Szabo G, Tome T, Borsos I. Probability currents and entropy production in nonequilibrium lattice systems. *Physical Review E.* 2010; 82: 011105.
[13] Gaveau B, Moreau M, Schulman LS. Generalized clausius relation and power dissipation in nonequilibrium stochastic systems. *Physical Review E.* 2009; 79: 010102.
[14] Lebowitz JL, Spohn H. A Gallavotti-cohen-type symmetry in the large deviation functional for stochastic dynamics. *Journal of Statistical Physics.* 1999; 95: 333.
[15] Andrieux D, Gaspar P. Fluctuation theorem for currents and schnakenberg network theory. *Journal of Statistical Physics.* 2007; 127: 107.
[16] Harris RJ, Schutz GM. Fluctuation theorems for stochastic dynamics. *Journal of Statistical Mechanics.* 2007; 2007(07): P07020.

[17] Tome T, de Oliveira MJ. Stochastic approach to equilibrium and nonequilibrium thermodynamics. *Physical Review E.* 2015; 9: 042140.
[18] Luo JL, Van den Broeck C, Nicolis G. Stability criteria and fluctuations around nonequilibrium states. *Journal of Physics B*. 1984; 56: 165.
[19] Mou CY, Luo JL, Nicolis G. Stochastic thermodynamics of nonequilibrium steady states in chemical reaction systems. *The Journal of Chemical Physics.* 1986; 84: 7011.
[20] Maes C, Netocny K. Time-reversal and entropy. *Journal of Statistical Physics.* 2003; 110: 269.
[21] Crochik L, Tome T. Entropy production in the majority-vote model. *Physical Review E.* 2005; 72: 057103.
[22] Asfaw M. Thermodynamic feature of a brownian heat engine operating between two heat baths. *Physical Review E.* 2014; 89: 012143.
[23] Asfaw M. Exact analytical thermodynamic expressions for a brownian heat engine. *Physical Review E.* 2015; 92: 032126.
[24] Brandner K, Bauer M, Schmid M, Seifert U. Coherence-enhanced efficiency of feedback-driven quantum engines. *New Journal of Physics.* 2015; 17: 065006.
[25] Gaveau B, Moreau M, Schulman LS. Constrained maximal power in small engines. *Physical Review E.* 2010; 82: 051109.
[26] Boukobza E, Tannor DJ. Three-level systems as amplifiers and attenuators: A thermodynamic analysis. *Physical Review Letters.* 2007; 98: 240601.
[27] Taye MA. Free energy and entropy production rate for a brownian particle that walks on overdamped medium. *Physical Review E.* 2016; 94: 032111.
[28] Taye MA. Entropy production and entropy extraction rates for a brownian particle that walks in underdamped medium. *Physical Review E.* 2020; 101: 012131.
[29] Ge H. Time reversibility and nonequilibrium thermodynamics of second-order stochastic processes. *Physical Review E.* 2014; 89: 022127.
[30] Lee HK, Kwon C, Park H. Fluctuation theorems and entropy production with odd-parity variables. *Physical Review Letters.* 2013; 110: 050602.
[31] Spinney RE, Ford IJ. Nonequilibrium thermodynamics of stochastic systems with odd and even variables. *Physical Review Letters.* 2012; 108: 170603.
[32] Celani A, Bo S, Eichhorn R, Aurell E. Anomalous thermodynamics at the microscale. *Physical Review Letters.* 2012; 109: 260603.
[33] Strasberg P, Esposito M. Non-Markovianity and negative entropy production rates. *Physical Review E.* 2019; 99: 012120.
[34] Manikandan SK, Gupta D, Krishnamurthy S. Inferring entropy production from short experiments. *Physical Review Letters.* 2020; 124: 120603.
[35] Skinner DJ, Dunkel J. Estimating entropy production from waiting time distributions. *Physical Review Letters.* 2021; 127: 198101.
[36] Otsubo S, Ito S, Dechant A, Sagawa T. Estimating entropy production by machine learning of short-time fluctuating currents. *Physical Review E.* 2020; 101: 062106.
[37] Vu TV, Vo VT, Hasegawa Y. Entropy production estimation with optimal current. *Physical Review E.* 2020; 101: 042138.
[38] Koyuk T, Seifert U. Operationally accessible bounds on fluctuations and entropy production in periodically driven systems. *Physical Review Letters.* 2019; 122: 230601.
[39] Taye MA. Exact time-dependent analytical solutions for entropy production rate in a system operating in a heat bath in which temperature varies linearly in space. *Physical Review E.* 2022; 105: 054126.
[40] Prigogine I. Time, Structure, and Fluctuations. *Science.* 1978; 201: 777.
[41] Ge H. Time reversibility and nonequilibrium thermodynamics of second-order stochastic processes. *Physical Review E.* 2014; 89: 022127.
[42] Goldhirsch I, Gefen Y. Analytic method for calculating properties of random walks on networks. *Physical Review A.* 1986; 33: 2583.
[43] Goldhirsch I, Gefen Y. Biased random walk on networks. *Physical Review A.* 1987; 35: 1317.
[44] Taye MA. Brownian motors arranged on nontrivial networks to achieve fast transport. *European Physical Journal B.* 2021; 94: 124.

Appendix A

In this Appendix we will give the expressions for $p_1(t)$, $p_2(t)$ and $p_3(t)$ as well as $V(t)$ for a Brownian particle that operates between the hot and cold baths. For the particle which is initially situated at site $i=2$, the time dependent normalized probability distributions after solving the rate equation $\frac{d\vec{p}}{dt}=\mathbf{P}\vec{p}$ are calculated as

$$p_1(t)=c_1\frac{a(2+\nu b)}{\mu\left(\mu+\left(a^2+\mu\right)\nu b\right)}+c_2e^{-\frac{\left(a+a^2\mu+\mu^2\right)t}{2a}}\left(-1+\frac{a(-1+a\mu)}{-\mu^2+a\nu b}\right), \tag{67}$$

$$p_2(t)=-c_3e^{\frac{1}{2}t(-2-\nu b)}-c_2\frac{a\,e^{-\frac{\left(a+a^2\mu+\mu^2\right)t}{2a}}(-1+a\mu)}{-\mu^2+a\nu b}+c_1\frac{\left(2a^2+\mu\right)}{\mu+\left(a^2+\mu\right)\nu b}, \tag{68}$$

$$p_3(t)=c_1+c_2e^{-\frac{\left(a+a^2\mu+\mu^2\right)t}{2a}}+c_3e^{\frac{1}{2}t(-2-\nu b)} \tag{69}$$

where

$$c_1=\frac{\mu\left(\mu+\left(a^2+\mu\right)\nu b\right)}{\left(a+a^2\mu+\mu^2\right)(2+\nu b)}, \tag{70}$$

$$c_2=-\frac{a}{\left(a+a^2\mu+\mu^2\right)\left(-1+\frac{a(-1+a\mu)}{-\mu^2+a\nu b}\right)}, \tag{71}$$

$$c_3=-\frac{\mu\left(\mu+a^2\nu b+\mu\nu b\right)}{\left(a+a^2\mu+\mu^2\right)(2+\nu b)}+\frac{a}{\left(a+a^2\mu+\mu^2\right)\left(-1+\frac{a(-1+a\mu)}{-\mu^2+a\nu b}\right)}. \tag{72}$$

Here $\sum_{i=1}^{3}p_i(t)=1$ revealing the probability distribution is normalized. In the limit of $t\to\infty$, we recapture the steady state probability distributions

$$p_1^s=\frac{a}{a+a^2\mu+\mu^2}, \tag{73}$$

$$p_2^s=\frac{\mu\left(2a^2+\mu\right)}{\left(a+a^2\mu+\mu^2\right)(2+b\nu)}, \tag{74}$$

$$p_3^s=\frac{\mu\left(\mu+b\left(a^2+\mu\right)\nu\right)}{\left(a+a^2\mu+\mu^2\right)(2+b\nu)}. \tag{75}$$

The velocity $V(t)$ at any time t is the difference between the forward $V_i^+(t)$ and backward $V_i^-(t)$ velocities at each site i

$$V(t) = \sum_{i=1}^{3} (V_i^+(t) - V_i^-(t))$$

$$= (p_1 P_{21} - p_2 P_{12}) + (p_2 P_{32} - p_3 P_{23}) + (p_3 P_{13} - p_1 P_{31}). \tag{76}$$

Exploiting Eq. (63), one can see that the particle attains a unidirectional current when $f = 0$ and $T_h > T_c$. For isothermal case $T_h = T_c$, the system sustains a non-zero velocity in the presence of load $f \neq 0$ as expected. Moreover, when $t \to \infty$, the velocity $V(t)$ increases with t and approaches the steady state velocity

$$V^s = 3 \frac{\mu \left(ba\nu - \frac{\mu}{a} \right)}{2(2 + \nu b) \left(1 + a\mu + \frac{\mu^2}{a} \right)}. \tag{77}$$

Appendix B

The expressions for $p_1(t)$, $p_2(t)$ and $p_3(t)$ as well as $V(t)$ are derived considering a Brownian particle that operates in a heat bath where its temperature decreases linearly along with the reaction coordinate. For the particle which is initially situated at site $i = 2$, the time-dependent normalized probability distributions after solving the rate equation $\frac{d\vec{p}}{dt} = \mathbf{P}\vec{p}$ are given as

$$p_1 = \frac{a_2(2+\nu)}{\mu_2^2 + a_1 a_2 \mu_1 \nu + \mu_2^2 \nu} c_1 + \left(-1 + \frac{-a_2 + a_1 a_2 \mu_1}{-\mu_2^2 + a_2 \nu}\right) e^{\left[t\left(\frac{-a_2 - a_1 a_2 \mu_1 - \mu_2^2}{2a_2}\right)\right]} c_2 \tag{78}$$

$$p_2 = -\frac{-2a_1 a_2 \mu_1 - \mu_2^2}{\mu_2^2 + a_1 a_2 \mu_1 \nu + \mu_2^2 \nu} c_1 - \frac{-a_2 + a_1 a_2 \mu_1}{-\mu_2^2 + a_2 \nu} e^{\left[t\left(\frac{-a_2 - a_1 a_2 \mu_1 - \mu_2^2}{2a_2}\right)\right]} c_2 - e^{\left[t\frac{1}{2}(-2-\nu)\right]} c_3 \tag{79}$$

$$p_3 = c_1 + e^{\left[t\left(\frac{-a_2 - a_1 a_2 \mu_1 - \mu_2^2}{2a_2}\right)\right]} c_2 + e^{\left[\frac{1}{2}(-2-\nu)t\right]} c_3 \tag{80}$$

where

$$c_1 = -\frac{-\mu_2^2 - a_1 a_2 \mu_1 \nu - \mu_2^2 \nu}{\left(a_2 + a_1 a_2 \mu_1 + \mu_2^2\right)(2+\nu)} \tag{81}$$

$$c_2 = -\frac{a_2\left(-\mu_2^2 + a_2 \nu\right)}{\left(a_2 + a_1 a_2 \mu_1 + \mu_2^2\right)\left(-a_2 + a_1 a_2 \mu_1 + \mu_2^2 - a_2 \nu\right)} \tag{82}$$

$$c_3 = \frac{\mu_2^2 - 2a_2 \nu + a_1 a_2 \mu_1 \nu + \mu_2^2 \nu - a_2 \nu^2}{(2+\nu)\left(a_{12} - a_1 a_2 \mu_1 - \mu_2^2 + a_2 \nu\right)}. \tag{83}$$

Once again, $\sum_{i=1}^{3} p_i(t) = 1$ revealing the probability distribution is normalized. When $t \to \infty$, the steady state probability distributions converge to

$$p_1^s = \frac{a_2}{(a_2 + a_1 a_2 \mu_1 + \mu_2^2)}, \tag{84}$$

$$p_2^s = \frac{(2a_1 a_2 \mu_1 + \mu_2^2)}{((a_2 + a_1 a_2 \mu_1 + \mu_2^2)(2+\nu))}, \tag{85}$$

$$p_3^s = \frac{(a_1 a_2 \mu_1 \nu + \mu_2^2(1+\nu))}{((a_2 + a_1 a_2 \mu_1 + \mu_2^2)(2+\nu))}. \tag{86}$$

The velocity $V(t)$ at any time t is the difference between the forward $V_i^+(t)$ and backward $V_i^-(t)$ velocities at each site i

$$V(t) = \sum_{i=1}^{3} (V_i^+(t) - V_i^-(t))$$

$$= (p_1 P_{21} - p_2 P_{12}) + (p_2 P_{32} - p_3 P_{23}) + (p_3 P_{13} - p_1 P_{31}). \tag{87}$$

In the limit $t \to \infty$, the velocity $V(t)$ increases with t and approaches to steady state velocity

$$V^s = \frac{(3(-\mu_2^2 + a_1 a_2 \mu_1 \nu))}{(2(a_2 + a_1 a_2 \mu_1 + \mu_2^2)(2+\nu))}. \tag{88}$$

Appendix C

The expressions for $p_1(t)$, $p_2(t)$, $p_3(t)$, $p_4(t)$ and $p_5(t)$ as well as $V(t)$ are derived considering a Brownian particle that operates in a cold and hot heat baths along with two dimensional lattice. For the particle which is initially situated at site $i=2$, the time-dependent normalized probability distributions after solving the rate equation $\frac{d\vec{p}}{dt}=\mathbf{P}\vec{p}$ are given as

$$p_1 = \frac{a(2+\nu b)}{a^2\mu\nu b+\mu^2(1+\nu b)}c_1+\left(-2+\frac{2a(-1+2a\mu)}{-2\mu^2+a\nu b}\right)\text{Exp}\left[t\left(-\frac{1}{2}-a\mu-\frac{\mu^2}{a}\right)\right]c_3 \tag{89}$$

$$P_2 = \frac{2a^2\mu+\mu^2}{a^2\mu\nu b+\mu^2(1+\nu b)}c_1+\left(-\frac{1}{\nu b}\right)\text{Exp}\left[-\frac{1}{2}t\right]c_2+\left(\frac{a-2a^2\mu}{-2\mu^2+a\nu b}\right)$$

$$\text{Exp}\left[t\left(-\frac{1}{2}-a\mu-\frac{\mu^2}{a}\right)\right]c_3-\text{Exp}\left[t\left(-1-\frac{\nu b}{2}\right)\right]c_5 \tag{90}$$

$$p_2' = \frac{2a^2\mu+\mu^2}{a^2\mu\nu b+\mu^2(1+\nu b)}c_1+\left(\frac{1}{\nu b}\right)\text{Exp}\left[-\frac{1}{2}t\right]c_2+\left(\frac{a-2a^2\mu}{-2\mu^2+a\nu b}\right)$$

$$\text{Exp}\left[t\left(-\frac{1}{2}-a\mu-\frac{\mu^2}{a}\right)\right]c_3-\text{Exp}\left[t\left(-1-\frac{\nu b}{2}\right)\right]c_4 \tag{91}$$

$$p_3 = c_1-\text{Exp}\left[-\frac{1}{2}t\right]c_2+\text{Exp}\left[t\left(-\frac{1}{2}-a\mu-\frac{\mu^2}{a}\right)\right]c_3+\text{Exp}\left[t\left(-1-\frac{\nu b}{2}\right)\right]c_5 \tag{92}$$

$$p_3' = c_1+\text{Exp}\left[-\frac{1}{2}t\right]c_2+\text{Exp}\left[t\left(-\frac{1}{2}-a\mu-\frac{\mu^2}{a}\right)\right]c_3+\text{Exp}\left[t\left(-1-\frac{\nu b}{2}\right)\right]c_4 \tag{93}$$

where

$$c_1 = -\frac{-\mu^2-a^2\mu\nu b-\mu^2\nu b}{(a+2a^2\mu+2\mu^2)(2+\nu b)} \tag{94}$$

$$c_2 = -\frac{\nu b}{2(1+\nu b)} \tag{95}$$

$$c_3 = -\frac{a\left(-2\mu^2+a\nu b\right)}{2(a+2a^2\mu+2\mu^2)(-a+2a^2\mu+2\mu^2-a\nu b)} \tag{96}$$

$$c_4 = -\frac{-\mu^2+a^2\mu\nu b}{(1+\nu b)(2+\nu b)(a-2a^2\mu-2\mu^2+a\nu b)} \tag{97}$$

$$c_5 = \frac{\mu^2-2a\nu b+3a^2\mu\nu b+4\mu^2\nu b-3a\nu^2b^2+2a^2\mu^2\nu b^2+2\mu^2\nu b^2-a\nu^3b^3}{(1+\nu b)(2+\nu b)(a-2a^2\mu-2\mu^2+a\nu b)} \tag{98}$$

Once again, $\sum_{i=1}^{3} p_i(t) = 1$ revealing the probability distribution is normalized. When $t \to \infty$, the steady state probability distributions converge to

$$p_1^s = \frac{a_2}{(a_2 + a_1 a_2 \mu_1 + \mu_2^2)}, \tag{99}$$

$$p_2^s = \frac{(2a_1 a_2 \mu_1 + \mu_2^2)}{((a_2 + a_1 a_2 \mu_1 + \mu_2^2)(2+\nu))}, \tag{100}$$

$$p_3^s = \frac{(a_1 a_2 \mu_1 \nu + \mu_2^2 (1+\nu))}{((a_2 + a_1 a_2 \mu_1 + \mu_2^2)(2+\nu))}. \tag{101}$$

The velocity $V(t)$ at any time t is the difference between the forward $V_i^+(t)$ and backward $V_i^-(t)$ velocities at each site i

$$\begin{aligned} V(t) &= \sum_{i=1}^{3} (V_i^+(t) - V_i^-(t)) \\ &= (p_1 P_{21} - p_2 P_{12}) + (p_2 P_{32} - p_3 P_{23}) + \\ &\quad (p_3 P_{13} - p_1 P_{31}) + (p_1 P'_{21} - p'_2 P'_{12}) + (p'_2 P'_{32} - p'_3 P'_{23})(p'_3 P'_{13} - p_1 P'_{31}) \end{aligned} \tag{102}$$

In the limit $t \to \infty$, the velocity $V(t)$ increases with t and approaches to steady state velocity

$$V^s = \frac{(3(-\mu_2^2 + a_1 a_2 \mu_1 \nu))}{(2(a_2 + a_1 a_2 \mu_1 + \mu_2^2)(2+\nu))}. \tag{103}$$

Appendix D

The expressions for $p_1(t)$, $p_2(t)$, $p_3(t)$, $p_4(t)$ and $p_5(t)$ as well as $V(t)$ are derived considering a Brownian particle that operates in a linearly decreasing heat baths along with two dimensional lattice.

For the particle which is initially situated at site $i = 2$, the time-dependent normalized probability distributions after solving the rate equation $\frac{d\vec{p}}{dt} = \mathbf{P}\vec{p}$ are given as

$$p_1 = \frac{a_2(2+\nu b)}{a_1 a_2 \mu_1 \nu b + {\mu_2}^2(1+\nu b)} c_1 + \left(-2 + \frac{2a_2(-1+2a_1\mu)}{-2{\mu_2}^2 + a_2 \nu b}\right) \mathrm{Exp}\left[t\left(-\frac{1}{2} - a_1\mu_1 - \frac{{\mu_2}^2}{a_2}\right)\right] c_3 \tag{104}$$

$$P_2 = \frac{2a_1 a_2 \mu_1 + \mu_2^2}{a_1 a_{21} \nu b + \mu_2^2(1+\nu b)} c_1 + \left(-\frac{1}{\nu b}\right) \mathrm{Exp}\left[-\frac{1}{2}t\right] c_2 + \left(\frac{a_2 - 2a_1 a_2 \mu_1}{-2\mu_2^2 + a_2 \nu b}\right)$$

$$\mathrm{Exp}\left[t\left(-\frac{1}{2} - a_1\mu_1 - \frac{\mu_2^2}{a_2}\right)\right] c_3 - \mathrm{Exp}\left[t\left(-1 - \frac{\nu b}{2}\right)\right] c_5 \tag{105}$$

$$p_2' = \frac{2a_1 a_2 \mu_+ \mu_2^2}{a_1 a_2 \mu_1 \nu b + \mu_2^2(1+\nu b)} c_1 + \left(\frac{1}{\nu b}\right) \mathrm{Exp}\left[-\frac{1}{2}t\right] c_2 + \left(\frac{a_2 - 2a_1 a_2 \mu}{-2\mu_2^2 + a_2 \nu b}\right)$$

$$\mathrm{Exp}\left[t\left(-\frac{1}{2} - a_1\mu_1 - \frac{\mu_2^2}{a_2}\right)\right] c_3 - \mathrm{Exp}\left[t\left(-1 - \frac{\nu b}{2}\right)\right] c_4 \tag{106}$$

$$p_3 = c_1 - \mathrm{Exp}\left[-\frac{1}{2}t\right] c_2 + \mathrm{Exp}\left[t\left(-\frac{1}{2} - a_1\mu_1 - \frac{\mu_2^2}{a_2}\right)\right] c_3 + \mathrm{Exp}\left[t\left(-1 - \frac{\nu b}{2}\right)\right] c_5 \tag{107}$$

$$p_3' = c_1 + \mathrm{Exp}\left[-\frac{1}{2}t\right] c_2 + \mathrm{Exp}\left[t\left(-\frac{1}{2} - a_1\mu_1 - \frac{\mu_2^2}{a_2}\right)\right] c_3 + \mathrm{Exp}\left[t\left(-1 - \frac{\nu b}{2}\right)\right] c_4 \tag{108}$$

where

$$c_1 = -\frac{-\mu_2^2 - a_1 a_2 \mu_1 \nu b - \mu_2^2 \nu b}{\left(a_2 + 2a_1 a_2 \mu_1 + 2\mu_2^2\right)(2+\nu b)} \tag{109}$$

$$c_2 = -\frac{\nu b}{2(1+\nu b)} \tag{110}$$

$$c_3 = -\frac{a_2\left(-2\mu_2^2 + a_2 \nu b\right)}{2\left(a_2 + 2a_1 a_2 \mu_1 + 2\mu_2^2\right)\left(-a_2 + 2a_1 a_2 \mu_1 + 2\mu_2^2 - a_2 \nu b\right)} \tag{111}$$

$$c_4 = -\frac{-\mu_2^2 + a_1 a_2 \mu_1 \nu b}{(1+\nu b)(2+\nu b)\left(a_2 - 2a_1 a_2 \mu_1 - 2\mu_2^2 + a_2 \nu b\right)} \tag{112}$$

$$c_5 = \frac{\mu_2^2 - 2a_2\nu b + 3a_1a_2\mu_1\nu b + 4\mu_2^2\nu b - 3a_2\nu^2b^2 + 2a_1a_2\mu_2^2\nu b^2 + 2\mu^2\nu b^2 - a_2\nu^3b^3}{(1+\nu b)(2+\nu b)\left(a_2 - 2a_1a_2\mu_1 - 2\mu_2^2 + a_2\nu b\right)} \tag{113}$$

Once again, $\sum_{i=1}^{3} p_i(t) = 1$ revealing the probability distribution is normalized. When $t \to \infty$, the steady state probability distributions converge to

$$p_1^s = \frac{a_2}{(a_2 + a_1a_2\mu_1 + \mu_2^2)}, \tag{114}$$

$$p_2^s = \frac{(2a_1a_2\mu_1 + \mu_2^2)}{((a_2 + a_1a_2\mu_1 + \mu_2^2)(2+\nu))}, \tag{115}$$

$$p_3^s = \frac{(a_1a_2\mu_1\nu + \mu_2^2(1+\nu))}{((a_2 + a_1a_2\mu_1 + \mu_2^2)(2+\nu))}. \tag{116}$$

The velocity $V(t)$ at any time t is the difference between the forward $V_i^+(t)$ and backward $V_i^-(t)$ velocities at each site i

$$\begin{aligned} V(t) =& \sum_{i=1}^{3}(V_i^+(t) - V_i^-(t)) \\ =& (p_1P_{21} - p_2P_{12}) + (p_2P_{32} - p_3P_{23}) + \\ & (p_3P_{13} - p_1P_{31}) + (p_1P'_{21} - p'_2P'_{12}) + (p'_2P'_{32} - p'_3P'_{23}) \\ & (p'_3P'_{13} - p_1P'_{31}) \end{aligned} \tag{117}$$

In the limit $t \to \infty$, the velocity $V(t)$ increases with t and approaches to steady state velocity

$$V^s = \frac{(3(-\mu_2^2 + a_1a_2\mu_1\nu))}{(2(a_2 + a_1a_2\mu_1 + \mu_2^2)(2+\nu))}. \tag{118}$$